Supplementary Information (SI) for Nanoscale.

Click Catalysis and DNA Conjugation using a Nanoscale DNA/Silver Cluster Pair

Caleb J. Setzler[a] and Jeffrey T. Petty[a,*]

[a]Department of Chemistry, Furman University, Greenville, SC 29613, United States

Table 1S: Summary of M/Z and Relative Intensities for the -4 (Entries 1-18) and -5 (Entries 19-39) of **Hx-1**/Ag_{10}^{6+}

	1	2	3	4	5	6	7	8	9	10
	M/Z_{obs}[a]	Int_{obs}[b]	M/Z_{pred}[c]	$Int_{pred}(Ag_{10}^{6+})$[d]	$Int_{pred}(Ag_{10}^{7+})$[e]	$Int_{pred}(Ag_{10}^{5+})$[f]	$\Delta M/Z$[g]	$\Delta Int(Ag_{10}^{6+})$[h]	$\Delta Int(Ag_{10}^{7+})$[i]	$\Delta Int(Ag_{10}^{5+})$[j]
1	1299.9774	0.08	1299.9784	0.01	0.03	0.00	0.78	0.06	0.05	0.08
2	1300.1770	0.08	1300.1788	0.03	0.08	0.01	1.42	0.05	0.00	0.06
3	1300.3776	0.18	1300.3786	0.08	0.12	0.03	0.75	0.10	0.05	0.15
4	1300.5769	0.19	1300.5789	0.12	0.25	0.08	1.54	0.07	0.06	0.12
5	1300.7715	0.35	1300.7787	0.25	0.35	0.12	5.57	0.11	0.00	0.23
6	1300.9788	0.45	1300.9790	0.35	0.55	0.25	0.13	0.10	0.10	0.20
7	1301.1754	0.60	1301.1789	0.55	0.68	0.35	2.68	0.06	0.08	0.25
8	1301.3776	0.76	1301.3791	0.68	0.86	0.55	1.13	0.08	0.10	0.22
9	1301.5779	0.87	1301.5791	0.86	0.94	0.68	0.88	0.01	0.07	0.19
10	1301.7773	0.95	1301.7792	0.94	1.00	0.86	1.45	0.01	0.05	0.09
11	1301.9788	**1.00**	1301.9792	**1.00**	0.96	0.94	0.32	0.00	0.04	0.06
12	1302.1783	0.96	1302.1793	0.96	0.87	1.00	0.80	0.00	0.09	0.04
13	1302.3778	0.83	1302.3794	0.87	0.73	0.96	1.24	0.04	0.10	0.13
14	1302.5790	0.69	1302.5795	0.73	0.57	0.87	0.41	0.03	0.12	0.18
15	1302.7786	0.57	1302.7797	0.57	0.42	0.73	0.81	0.00	0.15	0.16
16	1302.9794	0.43	1302.9798	0.42	0.28	0.57	0.29	0.02	0.15	0.14
17	1303.1796	0.34	1303.1799	0.28	0.18	0.42	0.25	0.05	0.16	0.08
18	1303.3790	0.21	1303.3801	0.18	0.11	0.28	0.84	0.03	0.10	0.07
19	1303.5800	0.15	1303.5803	0.11	0.06	0.18	0.22	0.04	0.09	0.03
20	1303.7806	0.11	1303.7805	0.06	0.03	0.11	0.07	0.05	0.08	0.01
21	1303.9791	0.08	1303.9808	0.03	0.01	0.06	1.27	0.05	0.07	0.02
22	1304.1831	0.06	1304.1810	0.01	0.01	0.03	1.60	0.05	0.06	0.03
23	1304.3788	0.06	1304.3813	0.01	0.00	0.01	1.92	0.05	0.05	0.04
24	1624.7155	0.01	1624.7246	0.00	0.00	0.00	5.61	0.01	0.01	0.01
25	1625.2189	0.03	1625.2248	0.01	0.03	0.00	3.65	0.02	0.01	0.03
26	1625.4707	0.05	1625.4754	0.03	0.08	0.01	2.87	0.02	0.03	0.03
27	1625.7214	0.10	1625.7251	0.08	0.12	0.03	2.25	0.03	0.02	0.08
28	1625.9734	0.16	1625.9754	0.12	0.25	0.08	1.25	0.03	0.09	0.08
29	1626.2241	0.29	1626.2252	0.25	0.35	0.12	0.70	0.04	0.07	0.16
30	1626.4744	0.39	1626.4755	0.35	0.55	0.25	0.69	0.04	0.15	0.15
31	1626.7245	0.59	1626.7254	0.55	0.68	0.35	0.57	0.04	0.10	0.23
32	1626.9756	0.72	1626.9757	0.68	0.86	0.55	0.03	0.04	0.14	0.18
33	1627.2255	0.89	1627.2256	0.86	0.94	0.68	0.08	0.03	0.06	0.20
34	1627.4750	0.96	1627.4758	0.94	1.00	0.86	0.49	0.02	0.04	0.10
35	1627.7252	**1.00**	1627.7258	**1.00**	0.96	0.94	0.39	0.00	0.04	0.06
36	1627.9762	0.96	1627.9760	0.96	0.87	1.00	0.12	0.00	0.09	0.04
37	1628.2253	0.86	1628.2261	0.87	0.73	0.96	0.49	0.01	0.14	0.09
38	1628.4758	0.72	1628.4762	0.73	0.57	0.87	0.27	0.01	0.15	0.15
39	1628.7253	0.57	1628.7264	0.57	0.42	0.73	0.66	0.00	0.16	0.15
40	1628.9762	0.42	1628.9766	0.42	0.28	0.57	0.21	0.01	0.14	0.15
41	1629.2264	0.29	1629.2267	0.28	0.18	0.42	0.21	0.01	0.11	0.12
42	1629.4761	0.20	1629.4770	0.18	0.11	0.28	0.52	0.02	0.09	0.09
43	1629.7269	0.12	1629.7272	0.11	0.06	0.18	0.18	0.02	0.07	0.05
44	1629.9783	0.08	1629.9775	0.06	0.03	0.11	0.52	0.02	0.05	0.03
45	1630.2266	0.05	1630.2278	0.03	0.01	0.06	0.71	0.02	0.04	0.01
46	1630.4729	0.04	1630.4781	0.01	0.01	0.03	3.18	0.02	0.03	0.01
47	1630.7207	0.03	1630.7285	0.01	0.00	0.01	4.76	0.03	0.03	0.02
48	1630.9696	0.03	1630.9789	0.00	0.00	0.01	5.67	0.03	0.03	0.03
49	1631.2194	0.04	1631.2293	0.00	0.00	0.00	6.06	0.04	0.04	0.04
							1.40	**0.02**	0.07	0.09

[a]Column 1: Observed M/Z values [b]Column 2: Observed and normalized intensities. The highlighted values (yellow) indicate the peak of the two distributions for the -4 and -5 charged complexes. [c]Column 3: Predicted M/Z values based on the molecular formula $[C_{175}H_{221}O_{113}N_{53}P_{18}Ag_{10}]^{-4}$ and $[C_{175}H_{220}O_{113}N_{53}P_{18}Ag_{10}]^{-5}$, respectively. [d]Column 4: Predicted intensities based on a Ag_{10}^{6+} adduct. [e]Column 5: Predicted intensities based on a Ag_{10}^{7+} adduct. [f]Column 6: Predicted intensities based on a Ag_{10}^{5+} adduct. [g]Column 7: Absolute differences in the observed and predicted M/Z values (|Column 1 – Column 3|). The observed average value of 1.40 ppm at the bottom of the column (red font) is within the precision of our instrument. [h]Column 8: Absolute differences in the observed and predicted intensities based on a Ag_{10}^{6+} adduct (|Column 2 – Column 4|) [i]Column 9: Absolute differences in the observed and predicted intensities based on a Ag_{10}^{5+} adduct (|Column 2 – Column 5|) [j]Column 10: Absolute differences in the observed and predicted intensities based on a Ag_{10}^{7+} adduct (|Column 2 – Column 6|) For Columns 8-10, the highlighted (in yellow) entries are the peak of the distributions for the -4 and -5 charged ions. For Columns 8-10, the red values at the bottom of the columns are the averages of the absolute differences. The small value for the Ag_{10}^{6+} adduct indicates this is the correct oxidation state for this cluster.

Table 2S: Summary of M/Z and Relative Intensities for the -4 (Entries 1-18) and -5 (Entries 19-39) of **Hx-1**/Ag_{10}^{6+}/N_3-C_3H_6-NH_2

	1	2	3	3	5	6	7	8	9	10
	M/Z_{obs}[a]	Int_{obs}[b]	M/Z_{pred}[c]	$Int_{pred}(Ag_{10}^{6+})$[d]	$Int_{pred}(Ag_{10}^{7+})$[e]	$Int_{pred}(Ag_{10}^{5+})$[f]	$\Delta M/Z$[g]	$\Delta Int(Ag_{10}^{6+})$	$\Delta Int(Ag_{10}^{7+})$	$\Delta Int(Ag_{10}^{5+})$
1	1320.4016	0.14	1320.3936	0.07	0.12	0.03	6.1	0.07	0.02	0.11
2	1320.5964	0.18	1320.5939	0.12	0.24	0.07	1.9	0.06	0.06	0.11
3	1320.7955	0.29	1320.7937	0.24	0.35	0.12	1.3	0.05	0.06	0.17
4	1320.9951	0.43	1320.9940	0.35	0.54	0.24	0.9	0.08	0.11	0.19
5	1321.1969	0.53	1321.1939	0.54	0.68	0.35	2.3	0.01	0.15	0.18
6	1321.3982	0.65	1321.3941	0.68	0.85	0.54	3.1	0.02	0.20	0.12
7	1321.5979	0.80	1321.5940	0.85	0.94	0.68	2.9	0.05	0.14	0.12
8	1321.7988	0.85	1321.7942	0.94	1.00	0.85	3.5	0.09	0.15	0.00
9	1321.9969	**1.00**	1321.9942	**1.00**	0.96	0.94	2.0	0.00	0.04	0.06
10	1322.1975	0.88	1322.1943	0.96	0.88	1.00	2.4	0.08	0.00	0.12
11	1322.3977	0.83	1322.3944	0.88	0.74	0.96	2.5	0.05	0.09	0.13
12	1322.5977	0.71	1322.5945	0.74	0.58	0.88	2.4	0.03	0.13	0.17
13	1322.7958	0.58	1322.7946	0.58	0.42	0.74	0.9	0.00	0.15	0.16
14	1322.9934	0.51	1322.9948	0.42	0.29	0.58	1.0	0.09	0.22	0.07
15	1323.1923	0.42	1323.1949	0.29	0.18	0.42	2.0	0.13	0.24	0.00
16	1323.3894	0.30	1323.3951	0.18	0.11	0.29	4.3	0.11	0.19	0.01
17	1323.5844	0.24	1323.5953	0.11	0.06	0.18	8.2	0.13	0.18	0.05
18	1323.7781	0.18	1323.7955	0.06	0.03	0.11	13.1	0.12	0.15	0.07
19	1650.7479	0.11	1650.7438	0.07	0.12	0.03	2.5	0.04	0.01	0.09
20	1651.0020	0.16	1650.9942	0.12	0.24	0.07	4.7	0.04	0.08	0.09
21	1651.2516	0.28	1651.2440	0.24	0.35	0.12	4.6	0.04	0.07	0.16
22	1651.5031	0.38	1651.4943	0.35	0.54	0.24	5.4	0.03	0.16	0.13
23	1651.7548	0.56	1651.7442	0.54	0.68	0.35	6.4	0.02	0.12	0.21
24	1652.0043	0.68	1651.9944	0.68	0.85	0.54	6.0	0.00	0.17	0.14
25	1652.2534	0.85	1652.2444	0.85	0.94	0.68	5.5	0.01	0.10	0.17
26	1652.5049	0.94	1652.4945	0.94	1.00	0.85	6.3	0.00	0.06	0.08
27	1652.7545	**1.00**	1652.7446	**1.00**	0.96	0.94	6.0	0.00	0.04	0.06
28	1653.0028	0.98	1652.9947	0.96	0.88	1.00	4.9	0.01	0.10	0.02
29	1653.2513	0.92	1653.2448	0.88	0.74	0.96	3.9	0.05	0.19	0.04
30	1653.5017	0.81	1653.4950	0.74	0.58	0.88	4.1	0.08	0.23	0.06
31	1653.7505	0.68	1653.7451	0.58	0.42	0.74	3.3	0.10	0.25	0.06
32	1653.9954	0.56	1653.9953	0.42	0.29	0.58	0.1	0.14	0.27	0.02
33	1654.2395	0.47	1654.2455	0.29	0.18	0.42	3.6	0.18	0.28	0.04
34	1654.4924	0.37	1654.4957	0.18	0.11	0.29	2.0	0.19	0.26	0.08
35	1654.7317	0.28	1654.7459	0.11	0.06	0.18	8.6	0.17	0.22	0.10
36	1654.9734	0.23	1654.9962	0.06	0.03	0.11	13.8	0.17	0.20	0.12
37	1655.2207	0.18	1655.2465	0.03	0.01	0.06	15.6	0.15	0.17	0.12
38	1655.4758	0.15	1655.4968	0.01	0.01	0.03	12.7	0.13	0.14	0.12
39	1655.7201	0.12	1655.7472	0.01	0.00	0.01	16.4	0.11	0.11	0.10
							5.1	**0.07**	**0.14**	**0.10**

[a]Column 1: Observed M/Z values [b]Column 2: Observed and normalized intensities. The highlighted values (yellow) indicate the peak of the two distributions for the -4 and -5 charged complexes. [c]Column 3: Predicted M/Z values based on the molecular formula $[C_{178}H_{229}O_{113}N_{57}P_{18}Ag_{10}]^{-4}$ and $[C_{178}H_{228}O_{113}N_{57}P_{18}Ag_{10}]^{-5}$, respectively. [d]Column 4: Predicted intensities based on a Ag_{10}^{6+} adduct. [e]Column 5: Predicted intensities based on a Ag_{10}^{7+} adduct. [f]Column 6: Predicted intensities based on a Ag_{10}^{5+} adduct. [g]Column 7: Absolute differences in the observed and predicted M/Z values (|Column 1 – Column 3|). The observed average value of 5.1 ppm at the bottom of the column (red font) is within the precision of our instrument. [h]Column 8: Absolute differences in the observed and predicted intensities based on a Ag_{10}^{6+} adduct (|Column 2 – Column 4|) [i]Column 9: Absolute differences in the observed and predicted intensities based on a Ag_{10}^{5+} adduct (|Column 2 – Column 5|) [j]Column 10: Absolute differences in the observed and predicted intensities based on a Ag_{10}^{7+} adduct (|Column 2 – Column 6|) For Columns 8-10, the highlighted (in yellow) entries are the peak of the distributions for the -4 and -5 charged ions. For Columns 8-10, the red values at the bottom of the columns are the averages of the absolute differences. The small value for the Ag_{10}^{6+} adduct indicates this is the correct oxidation state for this cluster.

Table 3S: Summary of M/Z and Relative Intensities for the -4 (Entries 1-21) and -5 (Entries 22-39) of **Hx-1**/Ag_{10}^{6+}/N_3-C_3H_6-OH

	1	2	3	4	5	6	7	8	9	10
	M/Z_{obs}[a]	Int_{obs}[b]	M/Z_{pred}[c]	$Int_{pred}(Ag_{10}^{6+})$[d]	$Int_{pred}(Ag_{10}^{7+})$[e]	$Int_{pred}(Ag_{10}^{5+})$[f]	$\Delta M/Z$[g]	$\Delta Int(Ag_{10}^{6+})$	$\Delta Int(Ag_{10}^{7+})$	$\Delta Int(Ag_{10}^{5+})$
1	1320.1920	0.17	1320.1902	0.01	0.03	0.00	1.36	0.16	0.15	0.17
2	1320.3959	0.10	1320.3906	0.03	0.07	0.01	4.00	0.07	0.02	0.08
3	1320.5892	0.18	1320.5904	0.07	0.12	0.03	0.89	0.11	0.06	0.16
4	1320.7867	0.20	1320.7907	0.12	0.24	0.07	3.01	0.08	0.04	0.13
5	1320.9878	0.34	1320.9905	0.24	0.35	0.12	2.07	0.10	0.01	0.22
6	1321.1896	0.43	1321.1908	0.35	0.54	0.24	0.88	0.08	0.11	0.19
7	1321.3939	0.61	1321.3907	0.54	0.68	0.35	2.43	0.07	0.07	0.26
8	1321.5898	0.71	1321.5909	0.68	0.85	0.54	0.80	0.03	0.14	0.17
9	1321.7882	0.87	1321.7909	0.85	0.94	0.68	2.00	0.01	0.07	0.19
10	1321.9899	0.95	1321.9910	0.94	1.00	0.85	0.82	0.01	0.05	0.10
11	1322.1902	1.00	1322.1910	1.00	0.96	0.94	0.62	0.00	0.04	0.06
12	1322.3911	0.94	1322.3911	0.96	0.88	1.00	0.03	0.02	0.07	0.06
13	1322.5891	0.86	1322.5912	0.88	0.74	0.96	1.60	0.01	0.13	0.10
14	1322.7911	0.72	1322.7913	0.74	0.58	0.88	0.17	0.02	0.14	0.16
15	1322.9908	0.60	1322.9915	0.58	0.42	0.74	0.49	0.02	0.18	0.13
16	1323.1915	0.53	1323.1916	0.42	0.29	0.58	0.06	0.10	0.24	0.05
17	1323.3950	0.36	1323.3917	0.29	0.18	0.42	2.47	0.07	0.17	0.07
18	1323.5906	0.27	1323.5919	0.18	0.11	0.29	0.98	0.09	0.16	0.02
19	1323.7921	0.19	1323.7921	0.11	0.06	0.18	0.01	0.08	0.13	0.00
20	1323.9904	0.12	1323.9923	0.06	0.03	0.11	1.44	0.06	0.09	0.01
21	1324.1956	0.16	1324.1925	0.03	0.01	0.06	2.31	0.13	0.14	0.10
22	1650.9858	0.14	1650.9898	0.07	0.12	0.03	2.42	0.06	0.02	0.11
23	1651.2416	0.19	1651.2402	0.12	0.24	0.07	0.87	0.07	0.05	0.12
24	1651.4927	0.31	1651.4900	0.24	0.35	0.12	1.64	0.07	0.04	0.19
25	1651.7426	0.43	1651.7403	0.35	0.54	0.24	1.41	0.08	0.11	0.19
26	1651.9921	0.59	1651.9902	0.54	0.68	0.35	1.16	0.05	0.09	0.24
27	1652.2427	0.74	1652.2404	0.68	0.85	0.54	1.40	0.06	0.11	0.20
28	1652.4950	0.91	1652.4904	0.85	0.94	0.68	2.80	0.05	0.03	0.23
29	1652.7455	0.94	1652.7405	0.94	1.00	0.85	3.00	0.00	0.06	0.09
30	1652.9926	1.00	1652.9906	1.00	0.96	0.94	1.22	0.00	0.04	0.06
31	1653.2418	0.98	1653.2407	0.96	0.88	1.00	0.64	0.02	0.11	0.02
32	1653.4976	0.91	1653.4908	0.88	0.74	0.96	4.09	0.03	0.17	0.05
33	1653.7477	0.76	1653.7410	0.74	0.58	0.88	4.06	0.02	0.18	0.12
34	1653.9923	0.61	1653.9911	0.58	0.42	0.74	0.71	0.03	0.18	0.13
35	1654.2385	0.51	1654.2413	0.42	0.29	0.58	1.69	0.09	0.22	0.07
36	1654.5001	0.38	1654.4915	0.29	0.18	0.42	5.20	0.09	0.19	0.05
37	1654.7467	0.25	1654.7417	0.18	0.11	0.29	3.02	0.06	0.14	0.04
38	1654.9937	0.14	1654.9919	0.11	0.06	0.18	1.07	0.04	0.08	0.04
39	1655.2317	0.18	1655.2422	0.06	0.03	0.11	6.34	0.12	0.15	0.07
							1.82	**0.06**	**0.11**	**0.11**

[a]Column 1: Observed M/Z values [b]Column 2: Observed and normalized intensities. The highlighted values (yellow) indicate the peak of the two distributions for the -4 and -5 charged complexes. [c]Column 3: Predicted M/Z values based on the molecular formula $[C_{178}H_{228}O_{114}N_{56}P_{18}Ag_{10}]^{-4}$ and $[C_{178}H_{227}O_{114}N_{56}P_{18}Ag_{10}]^{-5}$, respectively. [d]Column 4: Predicted intensities based on a Ag_{10}^{6+} adduct. [e]Column 5: Predicted intensities based on a Ag_{10}^{7+} adduct. [f]Column 6: Predicted intensities based on a Ag_{10}^{5+} adduct. [g]Column 7: Absolute differences in the observed and predicted M/Z values (|Column 1 – Column 3|). The observed average value of 1.82 ppm at the bottom of the column (red font) is within the precision of our instrument. [h]Column 8: Absolute differences in the observed and predicted intensities based on a Ag_{10}^{6+} adduct (|Column 2 – Column 4|) [i]Column 9: Absolute differences in the observed and predicted intensities based on a Ag_{10}^{5+} adduct (|Column 2 – Column 5|) [j]Column 10: Absolute differences in the observed and predicted intensities based on a Ag_{10}^{7+} adduct (|Column 2 – Column 6|) For Columns 8-10, the highlighted (in yellow) entries are the peak of the distributions for the -4 and -5 charged ions. For Columns 8-10, the red values at the bottom of the columns are the averages of the absolute differences. The small value for the Ag_{10}^{6+} adduct indicates this is the correct oxidation state for this cluster.

Table 4S: Summary of M/Z and Relative Intensities for the -4 (Entries 1-21) and -5 (Entries 22-39) of **Hx-1**/Ag_{10}^{6+}/N_3-C_3H_6-Biotin

	1	2	3	4	5	6	7	8	9	10
	M/Z_{obs}[a]	Int_{obs}[b]	M/Z_{pred}[c]	$Int_{pred}(Ag_{10}^{6+})$[d]	$Int_{pred}(Ag_{10}^{7+})$[e]	$Int_{pred}(Ag_{10}^{5+})$[f]	$\Delta M/Z$[g]	$\Delta Int(Ag_{10}^{6+})$	$\Delta Int(Ag_{10}^{7+})$	$\Delta Int(Ag_{10}^{5+})$
1	1380.4125	0.11	1380.4165	0.06	0.11	0.02	2.89	0.05	0.00	0.09
2	1380.6115	0.17	1380.6168	0.11	0.22	0.06	3.82	0.06	0.05	0.11
3	1380.8169	0.31	1380.8167	0.22	0.33	0.11	0.18	0.09	0.01	0.20
4	1381.0173	0.37	1381.0169	0.33	0.50	0.22	0.32	0.04	0.13	0.15
5	1381.2167	0.54	1381.2168	0.50	0.65	0.33	0.08	0.03	0.12	0.21
6	1381.4170	0.69	1381.4170	0.65	0.83	0.50	0.03	0.04	0.14	0.19
7	1381.6169	0.84	1381.6170	0.83	0.93	0.65	0.05	0.01	0.09	0.19
8	1381.8173	0.95	1381.8171	0.93	1.00	0.83	0.15	0.02	0.05	0.12
9	1382.0173	1.00	1382.0171	1.00	0.98	0.93	0.12	0.00	0.02	0.07
10	1382.2189	0.99	1382.2173	0.98	0.91	1.00	1.19	0.01	0.08	0.01
11	1382.4186	0.92	1382.4173	0.91	0.78	0.98	0.92	0.01	0.14	0.06
12	1382.6171	0.80	1382.6174	0.78	0.63	0.91	0.25	0.02	0.17	0.11
13	1382.8175	0.66	1382.8176	0.63	0.47	0.78	0.04	0.03	0.18	0.13
14	1383.0236	0.54	1383.0177	0.47	0.33	0.63	4.28	0.06	0.20	0.09
15	1383.2185	0.38	1383.2178	0.33	0.22	0.47	0.49	0.05	0.16	0.09
16	1383.4219	0.30	1383.4180	0.22	0.13	0.33	2.84	0.08	0.16	0.04
17	1383.6174	0.19	1383.6182	0.13	0.08	0.22	0.54	0.05	0.11	0.03
18	1383.8149	0.17	1383.8183	0.08	0.04	0.13	2.49	0.10	0.13	0.04
19	1384.0308	0.12	1384.0186	0.04	0.02	0.08	8.85	0.08	0.10	0.05
20	1725.7677	0.10	1725.7724	0.06	0.11	0.02	2.74	0.03	0.01	0.08
21	1726.0206	0.14	1726.0228	0.11	0.22	0.06	1.26	0.03	0.08	0.08
22	1726.2714	0.26	1726.2726	0.22	0.33	0.11	0.71	0.04	0.07	0.15
23	1726.5228	0.35	1726.5229	0.33	0.50	0.22	0.05	0.03	0.15	0.13
24	1726.7726	0.53	1726.7728	0.50	0.65	0.33	0.13	0.02	0.12	0.20
25	1727.0234	0.67	1727.0230	0.65	0.83	0.50	0.22	0.01	0.16	0.16
26	1727.2722	0.83	1727.2730	0.83	0.93	0.65	0.48	0.01	0.10	0.18
27	1727.5234	0.94	1727.5232	0.93	1.00	0.83	0.13	0.01	0.06	0.11
28	1727.7731	1.00	1727.7732	1.00	0.98	0.93	1.31	0.04	0.10	0.11
29	1728.0236	0.99	1728.0234	0.98	0.91	1.00	1.31	0.04	0.10	0.11
30	1728.2743	0.93	1728.2735	0.91	0.78	0.98	1.31	0.04	0.10	0.11
31	1728.5236	0.78	1728.5236	0.78	0.63	0.91	1.31	0.04	0.10	0.11
32	1728.7734	0.64	1728.7738	0.63	0.47	0.78	1.25	0.04	0.11	0.11
33	1729.0242	0.49	1729.0239	0.47	0.33	0.63	1.17	0.04	0.11	0.11
34	1729.2744	0.36	1729.2741	0.33	0.22	0.47	1.20	0.04	0.11	0.11
35	1729.5244	0.25	1729.5243	0.22	0.13	0.33	1.23	0.03	0.11	0.11
36	1729.7766	0.17	1729.7745	0.13	0.08	0.22	1.27	0.03	0.11	0.11
37	1730.0239	0.11	1730.0247	0.08	0.04	0.13	1.31	0.03	0.11	0.10
38	1730.2748	0.08	1730.2750	0.04	0.02	0.08	1.35	0.04	0.11	0.10
39	1730.5214	0.07	1730.5253	0.02	0.01	0.04	1.39	0.04	0.11	0.10
							1.30	**0.04**	**0.11**	**0.11**

[a]Column 1: Observed M/Z values [b]Column 2: Observed and normalized intensities. The highlighted values (yellow) indicate the peak of the two distributions for the -4 and -5 charged complexes. [c]Column 3: Predicted M/Z values based on the molecular formula $[C_{191}H_{249}O_{117}N_{59}SP_{18}Ag_{10}]^{-4}$ and $[C_{191}H_{248}O_{117}N_{59}SP_{18}Ag_{10}]^{-5}$, respectively. [d]Column 4: Predicted intensities based on a Ag_{10}^{6+} adduct. [e]Column 5: Predicted intensities based on a Ag_{10}^{7+} adduct. [f]Column 6: Predicted intensities based on a Ag_{10}^{5+} adduct. [g]Column 7: Absolute differences in the observed and predicted M/Z values (|Column 1 – Column 3|). The observed average value of 1.30 ppm at the bottom of the column (red font) is within the precision of our instrument. [h]Column 8: Absolute differences in the observed and predicted intensities based on a Ag_{10}^{6+} adduct (|Column 2 – Column 4|) [i]Column 9: Absolute differences in the observed and predicted intensities based on a Ag_{10}^{5+} adduct (|Column 2 – Column 5|) [j]Column 10: Absolute differences in the observed and predicted intensities based on a Ag_{10}^{7+} adduct (|Column 2 – Column 6|) For Columns 8-10, the highlighted (in yellow) entries are the peak of the distributions for the -4 and -5 charged ions. For Columns 8-10, the red values at the bottom of the columns are the averages of the absolute differences. The small value for the Ag_{10}^{6+} adduct indicates this is the correct oxidation state for this cluster.

Table 5S: Summary of M/Z and Relative Intensities for the -5 (Entries 1-9) and -4 (Entries 10-17) and -3 (Entries 18-26) of **Hx-1**/Ag_{10}^{6+}/CN^- in D_2O

	1	2	3	4	5	6	7	8
	M/Z_{obs}[a]	Int_{obs}[b]	M/Z_{pred}[c]	Int_{pred}[d]	$Int_{pred\text{-}D}$[e]	$\Delta M/Z$[f]	ΔInt[g]	ΔInt_D[h]
1	1086.9691	0.09	1086.9774	0.39	0.00	7.67	0.30	0.09
2	1087.1743	0.48	1087.1780	0.85	0.39	3.41	0.37	0.09
3	1087.3755	0.86	1087.3786	1.00	0.85	2.80	0.14	0.01
4	1087.5754	1.00	1087.5791	0.84	1.00	3.37	0.16	0.00
5	1087.7742	0.85	1087.7796	0.57	0.84	4.96	0.28	0.00
6	1087.9769	0.55	1087.9801	0.32	0.57	2.94	0.23	0.01
7	1088.1770	0.33	1088.1806	0.16	0.32	3.31	0.18	0.01
8	1088.3795	0.18	1088.3811	0.07	0.16	1.47	0.11	0.02
9	1088.5814	0.13	1088.5816	0.03	0.07	0.17	0.10	0.06
10	1358.9747	0.11	1358.9736	0.39	0.00	0.79	0.28	0.11
11	1359.2273	0.50	1359.2243	0.85	0.39	2.19	0.35	0.11
12	1359.4784	0.90	1359.4750	1.00	0.85	2.50	0.10	0.05
13	1359.7286	1.00	1359.7257	0.84	1.00	2.16	0.16	0.00
14	1359.9783	0.84	1359.9763	0.57	0.84	1.46	0.28	0.00
15	1360.2296	0.57	1360.2269	0.32	0.57	1.96	0.25	0.01
16	1360.4796	0.34	1360.4776	0.16	0.32	1.49	0.19	0.02
17	1360.7317	0.19	1360.7282	0.07	0.16	2.58	0.12	0.03
18	1812.3077	0.11	1812.3006	0.39	0.00	3.93	0.28	0.11
19	1812.6486	0.43	1812.6349	0.85	0.39	7.58	0.42	0.03
20	1812.9767	0.82	1812.9691	1.00	0.85	4.19	0.18	0.03
21	1813.3069	1.00	1813.3033	0.84	1.00	1.98	0.16	0.00
22	1813.6401	0.84	1813.6375	0.57	0.84	1.43	0.28	0.00
23	1813.9747	0.56	1813.9717	0.32	0.57	1.66	0.24	0.00
24	1814.3063	0.33	1814.3059	0.16	0.32	0.25	0.18	0.01
25	1814.6498	0.19	1814.6400	0.07	0.16	2.76	0.22	0.03
26	1814.9845	0.10	1814.9742	0.03	0.07	2.76	0.22	0.03
						2.76	0.22	**0.03**

[a]Column 1: Observed M/Z values [b]Column 2: Observed and normalized intensities. The highlighted values (yellow) indicate the peak of the two distributions for the -3, -4 and -5 charged complexes. [c]Column 3: Predicted M/Z values based on the molecular formulas and $[C_{175}H_{228}O_{113}N_{53}P_{18}]^{-3}$, $[C_{175}H_{227}O_{113}N_{53}P_{18}]^{-4}$, and $[C_{175}H_{226}O_{113}N_{53}P_{18}]^{-5}$ for the fully protonated DNA and $[C_{175}H_{227}DO_{113}N_{53}P_{18}]^{-3}$, $[C_{175}H_{226}DO_{113}N_{53}P_{18}]^{-4}$, and $[C_{175}H_{225}DO_{113}N_{53}P_{18}]^{-5}$ for the singly deuterated DNA. [d]Column 4: Predicted intensities based on a fully protonated **Hx-1**. [e]Column 5: Predicted intensities based on a singly deuterated **Hx-1**. [f]Column 6: Absolute differences in the observed and predicted M/Z values (|Column 1 – Column 3|). The observed average value of 2.76 ppm at the bottom of the column (red font) is within the precision of our instrument. [g]Column 7: Absolute differences in the observed and predicted intensities based on a fully protonated **Hx-1**. (|Column 2 – Column 4|) [h]Column 8: Absolute differences in the observed and predicted intensities based on a singly deuterated **Hx-1** (|Column 2 – Column 5|).

Table 6S: Summary of M/Z and Relative Intensities for the -5 (Entries 1-10) and -4 (Entries 11-19) and -3 (Entries 20-29) of **Hx-1**/Ag_{10}^{6+}/CN^- in H_2O

	1	2	3	4	5	6	7	8
	M/Z_{obs}[a]	Int_{obs}[b]	M/Z_{pred}[c]	Int_{pred}[d]	$Int_{pred\text{-}D}$[e]	$\Delta M/Z$[f]	ΔInt[g]	ΔInt_D[h]
1	1086.7484	0.05	1086.7759	0.00	0.00	25.28	0.05	0.05
2	1086.9728	0.42	1086.9774	0.39	0.00	4.27	0.03	0.42
3	1087.1741	0.86	1087.1780	0.85	0.39	3.60	0.01	0.47
4	1087.3749	1.00	1087.3786	1.00	0.85	3.36	0.00	0.15
5	1087.5762	0.87	1087.5791	0.84	1.00	2.64	0.02	0.13
6	1087.7754	0.58	1087.7796	0.57	0.84	3.85	0.02	0.26
7	1087.9763	0.34	1087.9801	0.32	0.57	3.49	0.02	0.23
8	1088.1780	0.18	1088.1806	0.16	0.32	2.39	0.02	0.14
9	1088.3794	0.09	1088.3811	0.07	0.16	1.56	0.03	0.06
10	1088.5906	0.07	1088.5816	0.03	0.07	8.28	0.05	0.00
11	1358.7305	0.04	1358.7217	0.00	0.00	6.51	0.04	0.04
12	1358.9763	0.44	1358.9736	0.39	0.00	1.97	0.04	0.44
13	1359.2262	0.87	1359.2243	0.85	0.39	1.38	0.03	0.48
14	1359.4774	1.00	1359.4750	1.00	0.85	1.77	0.00	0.15
15	1359.7278	0.86	1359.7257	0.84	1.00	1.57	0.01	0.14
16	1359.9781	0.58	1359.9763	0.57	0.84	1.32	0.02	0.26
17	1360.2291	0.34	1360.2269	0.32	0.57	1.59	0.02	0.22
18	1360.4788	0.18	1360.4776	0.16	0.32	0.90	0.02	0.14
19	1360.7299	0.09	1360.7282	0.07	0.16	1.26	0.02	0.07
20	1812.0072	0.01	1811.9646	0.00	0.00	23.49	0.01	0.01
21	1812.3123	0.34	1812.3006	0.39	0.00	6.47	0.05	0.34
22	1812.6417	0.76	1812.6349	0.85	0.39	3.77	0.08	0.37
23	1812.9717	1.00	1812.9691	1.00	0.85	1.43	0.00	0.15
24	1813.3073	0.84	1813.3033	0.84	1.00	2.20	0.00	0.16
25	1813.6444	0.55	1813.6375	0.57	0.84	3.80	0.01	0.29
26	1813.9744	0.31	1813.9717	0.32	0.57	1.50	0.01	0.26
27	1814.3068	0.15	1814.3059	0.16	0.32	0.52	0.00	0.16
28	1814.6475	0.08	1814.6400	0.07	0.16	4.13	0.01	0.08
29	1814.9812	0.04	1814.9742	0.03	0.07	3.87	0.02	0.03
						4.42	**0.02**	**0.20**

[a]Column 1: Observed M/Z values [b]Column 2: Observed and normalized intensities. The highlighted values (yellow) indicate the peak of the two distributions for the -3, -4 and -5 charged complexes. [c]Column 3: Predicted M/Z values based on the molecular formulas and $[C_{175}H_{228}O_{113}N_{53}P_{18}]^{-3}$, $[C_{175}H_{227}O_{113}N_{53}P_{18}]^{-4}$, and $[C_{175}H_{226}O_{113}N_{53}P_{18}]^{-5}$ for the fully protonated DNA and $[C_{175}H_{227}DO_{113}N_{53}P_{18}]^{-3}$, $[C_{175}H_{226}DO_{113}N_{53}P_{18}]^{-4}$, and $[C_{175}H_{225}DO_{113}N_{53}P_{18}]^{-5}$ for the singly deuterated DNA. [d]Column 4: Predicted intensities based on a fully protonated **Hx-1**. [e]Column 5: Predicted intensities based on a singly deuterated **Hx-1**. [f]Column 6: Absolute differences in the observed and predicted M/Z values (|Column 1 – Column 3|). The observed average value of 4.42 ppm at the bottom of the column (red font) is within the precision of our instrument. [g]Column 7: Absolute differences in the observed and predicted intensities based on a fully protonated **Hx-1**. (|Column 2 – Column 4|) [h]Column 8: Absolute differences in the observed and predicted intensities based on a singly deuterated **Hx-1** (|Column 2 – Column 5|).

Table 7S: Summary of M/Z and Relative Intensities for the -5 (Entries 1-11) and -4 (Entries 12-23) and -3 (Entries 24-33) of **1**/Ag_{10}^{6+}/CN^- in D_2O

	1	2	3	4	5	6	7	8
	M/Z_{obs}[a]	Int_{obs}[b]	M/Z_{pred}[c]	Int_{pred}[d]	$Int_{pred\text{-}D}$[e]	ΔM/Z[f]	ΔInt[g]	ΔInt_D[h]
1	1054.7461	0.06	1054.7701	0.00	0.00	22.74	0.06	0.06
2	1054.9674	0.44	1054.9717	0.42	0.00	4.03	0.02	0.44
3	1055.1683	0.87	1055.1722	0.87	0.42	3.72	0.00	0.46
4	1055.3693	**1.00**	1055.3728	**1.00**	0.87	3.27	0.00	0.13
5	1055.5701	0.87	1055.5733	0.82	**1.00**	3.01	0.05	0.13
6	1055.7698	0.59	1055.7738	0.54	0.82	3.78	0.05	0.23
7	1055.9708	0.34	1055.9743	0.29	0.54	3.31	0.05	0.19
8	1056.1710	0.20	1056.1748	0.14	0.29	3.59	0.06	0.10
9	1056.3723	0.10	1056.3753	0.06	0.14	2.83	0.04	0.04
10	1056.5708	0.07	1056.5758	0.02	0.06	4.71	0.05	0.01
11	1056.7673	0.03	1056.7763	0.01	0.02	8.48	0.03	0.01
12	1318.7279	0.04	1318.7144	0.00	0.00	10.21	0.04	0.04
13	1318.9686	0.45	1318.9664	0.42	0.00	1.68	0.03	0.45
14	1319.2194	0.87	1319.2171	0.87	0.42	1.75	0.00	0.45
15	1319.4695	**1.00**	1319.4678	**1.00**	0.87	1.32	0.00	0.13
16	1319.7198	0.85	1319.7184	0.82	**1.00**	1.05	0.03	0.15
17	1319.9702	0.59	1319.9691	0.54	0.82	0.86	0.05	0.23
18	1320.2211	0.35	1320.2197	0.29	0.54	1.07	0.06	0.19
19	1320.4717	0.19	1320.4703	0.14	0.29	1.05	0.05	0.10
20	1320.7220	0.10	1320.7209	0.06	0.14	0.81	0.04	0.04
21	1320.9716	0.05	1320.9715	0.02	0.06	0.05	0.03	0.01
22	1321.2220	0.03	1321.2222	0.01	0.02	0.11	0.02	0.00
23	1758.6714	0.01	1758.6217	0.00	0.00	28.28	0.01	0.01
24	1758.9690	0.35	1758.9576	0.42	0.00	6.48	0.06	0.35
25	1759.3005	0.79	1759.2919	0.87	0.42	4.90	0.08	0.38
26	1759.6307	**1.00**	1759.6261	**1.00**	0.87	2.61	0.00	0.13
27	1759.9648	0.86	1759.9603	0.82	**1.00**	2.55	0.04	0.14
28	1760.2992	0.57	1760.2945	0.54	0.82	2.67	0.03	0.26
29	1760.6305	0.32	1760.6287	0.29	0.54	1.04	0.03	0.21
30	1760.9679	0.17	1760.9628	0.14	0.30	2.87	0.03	0.13
31	1761.2981	0.09	1761.2970	0.06	0.14	0.62	0.03	0.05
32	1761.6373	0.05	1761.6312	0.02	0.06	3.49	0.03	0.01
33	1761.9739	0.03	1761.9653	0.01	0.02	4.89	0.02	0.01
						4.36	**0.03**	**0.16**

[a]Column 1: Observed M/Z values [b]Column 2: Observed and normalized intensities. The highlighted values (yellow) indicate the peak of the two distributions for the -3, -4 and -5 charged complexes. [c]Column 3: Predicted M/Z values based on the molecular formulas $[C_{169}H_{219}O_{110}N_{53}P_{17}]^{-3}$, $[C_{169}H_{218}O_{110}N_{53}P_{17}]^{-4}$, and $[C_{169}H_{217}O_{110}N_{53}P_{17}]^{-5}$ for the fully protonated DNA and $[C_{169}H_{218}DO_{110}N_{53}P_{17}]^{-3}$, $[C_{169}H_{217}DO_{110}N_{53}P_{17}]^{-4}$, and $[C_{169}H_{216}DO_{110}N_{53}P_{17}]^{-5}$ for the singly deuterated DNA. [d]Column 4: Predicted intensities based on a fully protonated **1**. [e]Column 5: Predicted intensities based on a singly deuterated **1**. [f]Column 6: Absolute differences in the observed and predicted M/Z values (|Column 1 – Column 3|). The observed average value of 4.36 ppm at the bottom of the column (red font) is within the precision of our instrument. [g]Column 7: Absolute differences in the observed and predicted intensities based on a fully protonated **1**. (|Column 2 – Column 4|) [h]Column 8: Absolute differences in the observed and predicted intensities based on a singly deuterated **1** (|Column 2 – Column 5|).

Table 8S: Summary of M/Z and Relative Intensities for the -5 (Entries 1-10) and -4 (Entries 11-19) and -3 (Entries 20-29) of **Hx-1**/CN^- in D_2O

	1	2	3	4	5	6	7	8
	M/Z_{obs}[a]	Int_{obs}[b]	M/Z_{pred}[c]	Int_{pred}[d]	$Int_{pred\text{-}D}$[e]	ΔM/Z[f]	ΔInt[g]	ΔInt_D[h]
1	1086.7208	0.12	1086.7759	0.00	0.00	50.67	0.12	0.12
2	1086.9724	0.36	1086.9774	0.39	0.00	4.64	0.03	0.36
3	1087.1736	0.82	1087.1780	0.85	0.39	4.06	0.03	0.43
4	1087.3759	**1.00**	1087.3786	**1.00**	0.85	2.44	0.00	0.15
5	1087.5751	0.95	1087.5791	0.84	**1.00**	3.65	0.11	0.05
6	1087.7732	0.70	1087.7796	0.57	0.84	5.87	0.14	0.14
7	1087.9760	0.40	1087.9801	0.32	0.57	3.77	0.08	0.17
8	1088.1781	0.21	1088.1806	0.16	0.32	2.30	0.06	0.11
9	1088.3784	0.12	1088.3811	0.07	0.16	2.48	0.05	0.04
10	1088.5780	0.09	1088.5816	0.03	0.07	3.30	0.06	0.02
11	1358.7218	0.02	1358.7217	0.00	0.00	0.10	0.02	0.02
12	1358.9740	0.37	1358.9736	0.39	0.00	0.28	0.02	0.37
13	1359.2251	0.81	1359.2243	0.85	0.39	0.57	0.04	0.42
14	1359.4760	**1.00**	1359.4750	**1.00**	0.85	0.74	0.00	0.15
15	1359.7260	0.90	1359.7257	0.84	**1.00**	0.25	0.05	0.10
16	1359.9767	0.65	1359.9763	0.57	0.84	0.29	0.08	0.20
17	1360.2269	0.38	1360.2269	0.32	0.57	0.03	0.06	0.18
18	1360.4780	0.20	1360.4776	0.16	0.32	0.32	0.04	0.12
19	1360.7296	0.10	1360.7282	0.07	0.16	1.04	0.03	0.05
20	1812.0123	0.01	1811.9646	0.00	0.00	26.30	0.01	0.01
21	1812.3044	0.34	1812.3006	0.39	0.00	2.11	0.05	0.34
22	1812.6399	0.76	1812.6349	0.85	0.39	2.78	0.08	0.37
23	1812.9741	**1.00**	1812.9691	**1.00**	0.85	2.76	0.00	0.15
24	1813.3046	0.91	1813.3033	0.84	**1.00**	0.71	0.07	0.09
25	1813.6367	0.66	1813.6375	0.57	0.84	0.44	0.09	0.19
26	1813.9707	0.38	1813.9717	0.32	0.57	0.54	0.07	0.18
27	1814.3026	0.22	1814.3059	0.16	0.32	1.79	0.07	0.10
28	1814.6400	0.12	1814.6400	0.07	0.16	0.01	0.05	0.04
29	1814.9807	0.07	1814.9742	0.03	0.07	3.60	0.04	0.00
						4.41	**0.05**	**0.16**

[a]Column 1: Observed M/Z values [b]Column 2: Observed and normalized intensities. The highlighted values (yellow) indicate the peak of the two distributions for the -3, -4 and -5 charged complexes. [c]Column 3: Predicted M/Z values based on the molecular formulas $[C_{175}H_{228}O_{113}N_{53}P_{18}]^{-3}$, $[C_{175}H_{227}O_{113}N_{53}P_{18}]^{-4}$, and $[C_{175}H_{226}O_{113}N_{53}P_{18}]^{-5}$ for the fully protonated DNA and $[C_{175}H_{227}DO_{113}N_{53}P_{18}]^{-3}$, $[C_{175}H_{226}DO_{113}N_{53}P_{18}]^{-4}$, and $[C_{175}H_{225}DO_{113}N_{53}P_{18}]^{-5}$ for the singly deuterated DNA. [d]Column 4: Predicted intensities based on a fully protonated **Hx-1**. [e]Column 5: Predicted intensities based on a singly deuterated **Hx-1**. [f]Column 6: Absolute differences in the observed and predicted M/Z values (|Column 1 – Column 3|). The observed average value of 4.41 ppm at the bottom of the column (red font) is within the precision of our instrument. [g]Column 7: Absolute differences in the observed and predicted intensities based on a fully protonated **Hx-1**. (|Column 2 – Column 4|) [h]Column 8: Absolute differences in the observed and predicted intensities based on a singly deuterated **Hx-1** (|Column 2 – Column 5|).

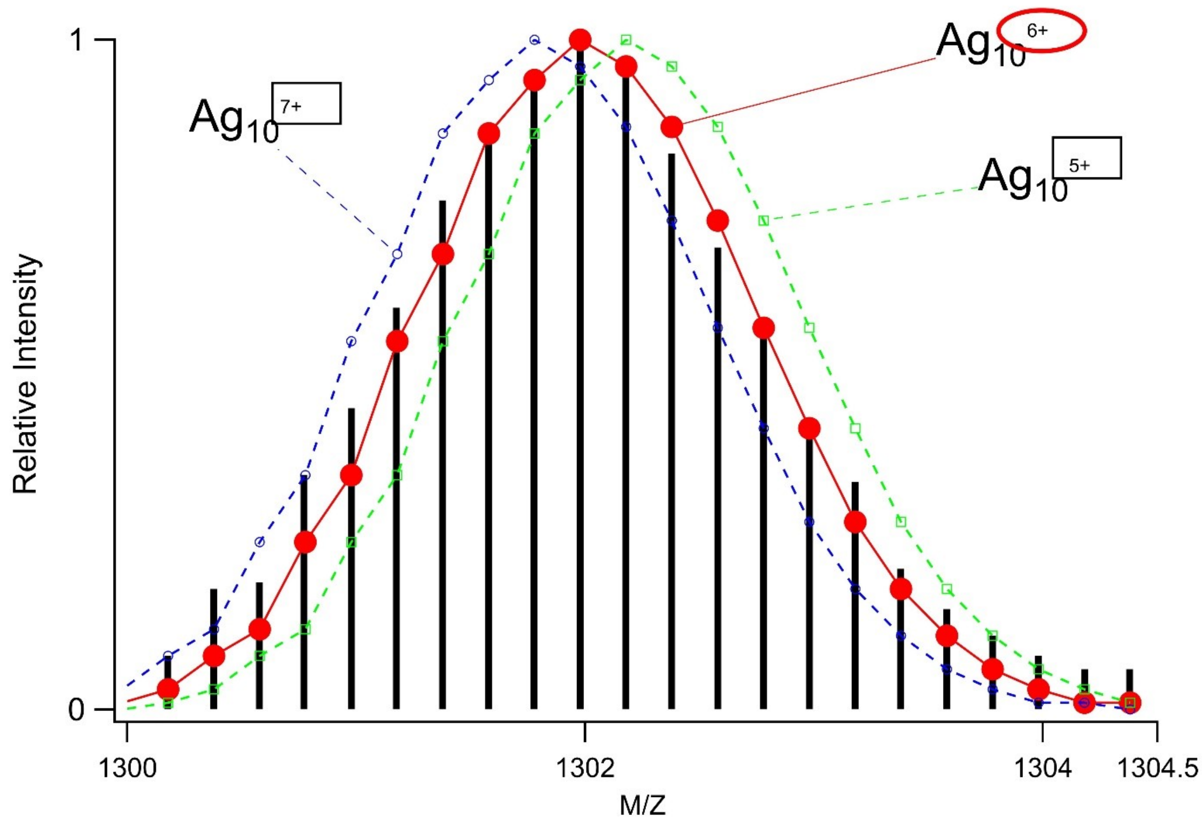

Figure 1S: Isotope models for based on the formulas $[(C_{175}H_{\underline{221}}N_{53}O_{113}P_{18})^{-10}(Ag_{10})^{6+}]^{-4}$ (red closed circles), $[(C_{175}H_{\underline{220}}N_{53}O_{113}P_{18})^{-10}(Ag_{10})^{7+}]^{-4}$ (blue open circles), and $[(C_{175}H_{\underline{222}}N_{53}O_{113}P_{18})^{-10}(Ag_{10})^{6+}]^{-4}$(green closed squares). Underlined subscripts emphasize the numbers of H^+, which are used to determine the oxidation state of the Ag_{10}. These charges are emphasized by black boxes and a red circle. The black sticks represent the experimental spectrum, which is best described by the Ag_{10}^{6+} distribution (red).

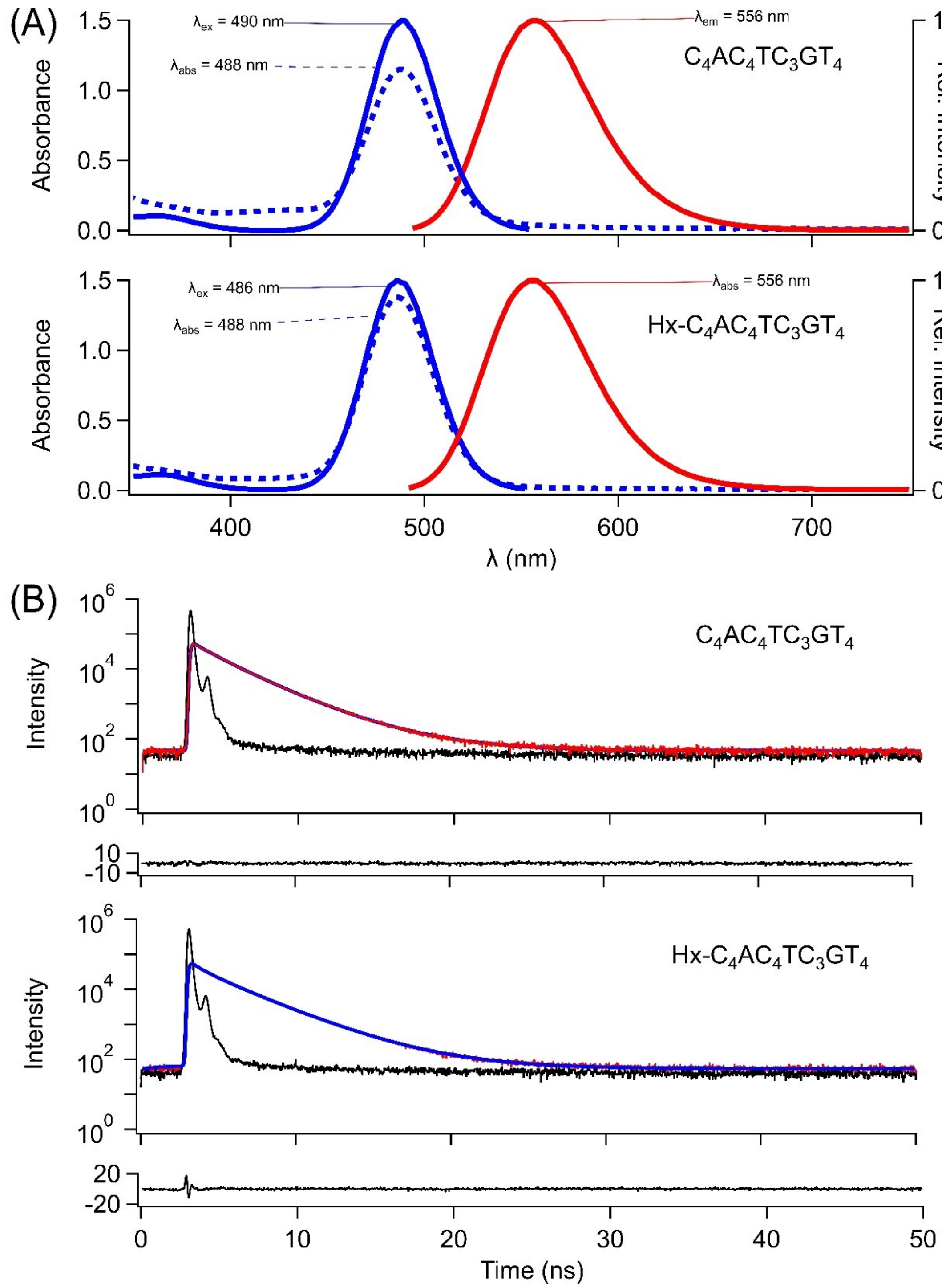

Figure S2: (A) Absorption (blue dotted), excitation (blue solid), and emission (red solid) spectra of $C_4AC_4TC_3GT_4/Ag_{10}^{6+}$ (top) and Hx-$C_4AC_4TC_3GT_4/Ag_{10}^{6+}$ (bottom) complexes. Similar λ_{max} values for absorption and fluorescence, overlapping absorption and excitation spectra, and comparable absorbances indicate similar binding sites for the Ag_{10}^{6+} adducts with both strands. (B) Fluorescence decays (red), IRF (black), and model results (blue) for $C_4AC_4TC_3GT_4/Ag_{10}^{6+}$ (top) and Hx-$C_4AC_4TC_3GT_4/Ag_{10}^{6+}$ (bottom) complexes. Residuals are provided below each decay. Similar lifetimes of 2.02 and 2.22 ns, respectively, also indicate similar binding sites for the Ag_{10}^{6+} adducts with both strands.

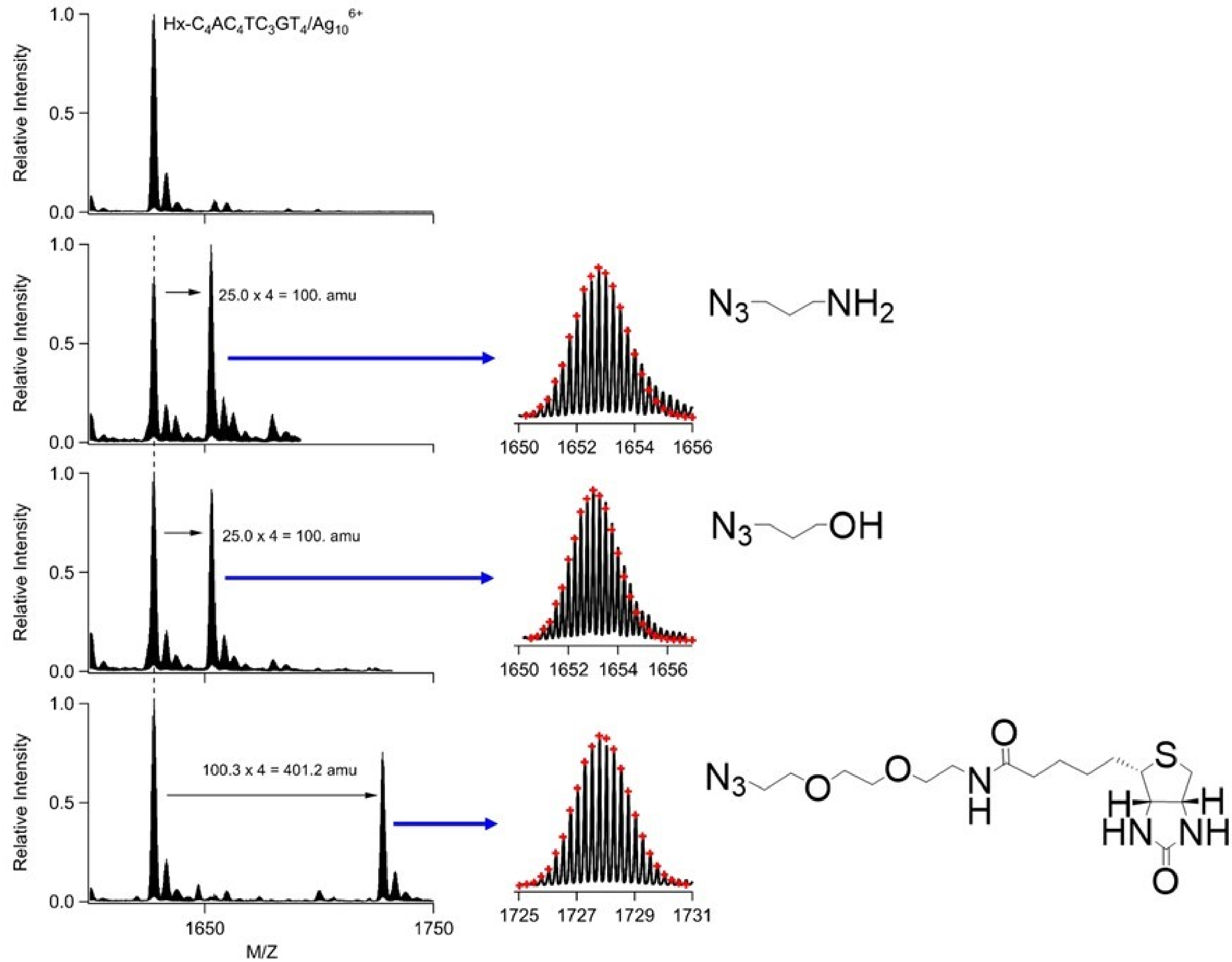

Figure 3S Mass spectra of the -4 charged Hx-$C_4AC_4TC_3GT_4$ complexes with no azide, N_3-C_3H_6-NH_2 (100.12 amu), N_3-C_3H_6-OH (100.11 amu), and N_3-$C_6H_{12}O_2$-$C_{10}H_{16}N_3O_2S$ (Biotin) (400.5 amu), respectively (top to bottom, respectively). The dashed line emphasizes the unreacted Hx-$C_4AC_4TC_3GT_4/Ag_{10}^{6+}$. The M/Z shift due to the azides are emphasized by the black arrows. The panels to the right of each spectrum show the isotopic fine structure that determined the molecular formulas (see Tables 2S – 4S).

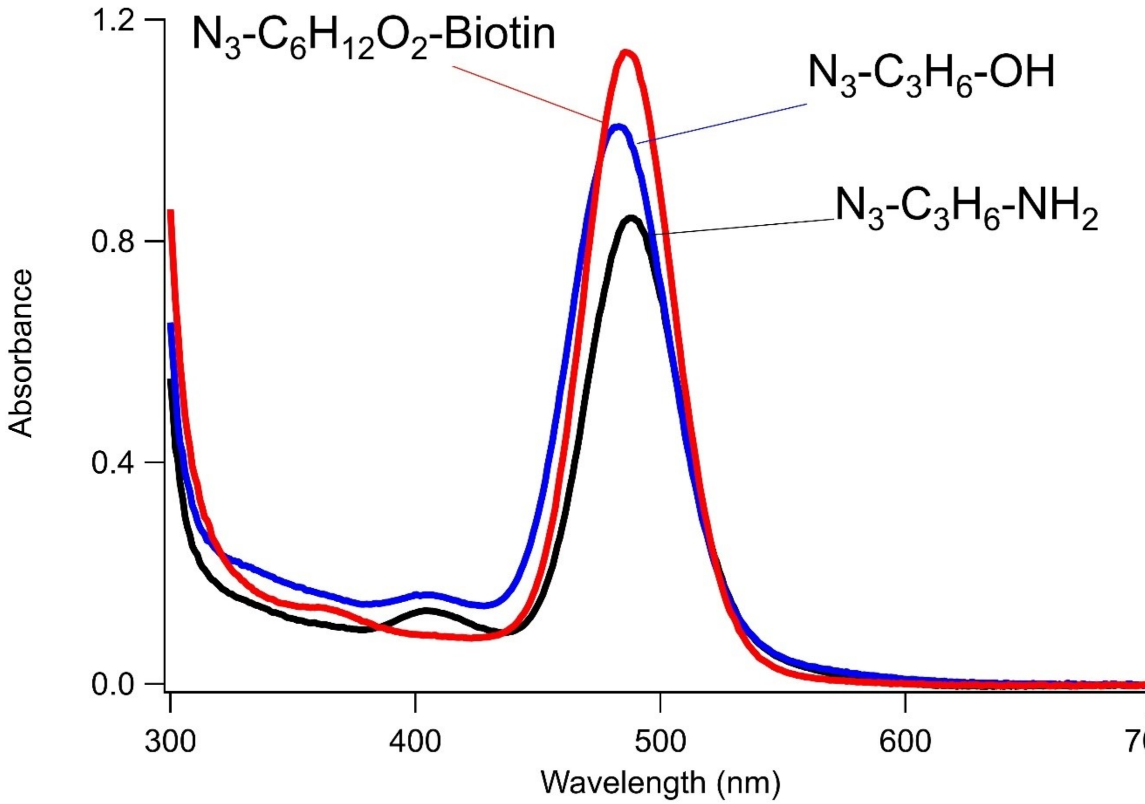

Figure 4S: Absorption spectra of Hx-$C_4AC_4TC_3GT_4/Ag_{10}^{6+}$ with N_3-C_3H_6-NH_2 (black) with λ_{max} = 488 nm, N_3-C_3H_6-OH (blue) with λ_{max} = 484 nm, and N_3-$C_6H_{12}O_2$-Biotin (red) with λ_{max} = 486 nm. Similar λ_{max} values indicate that the clusters have similar binding sites.

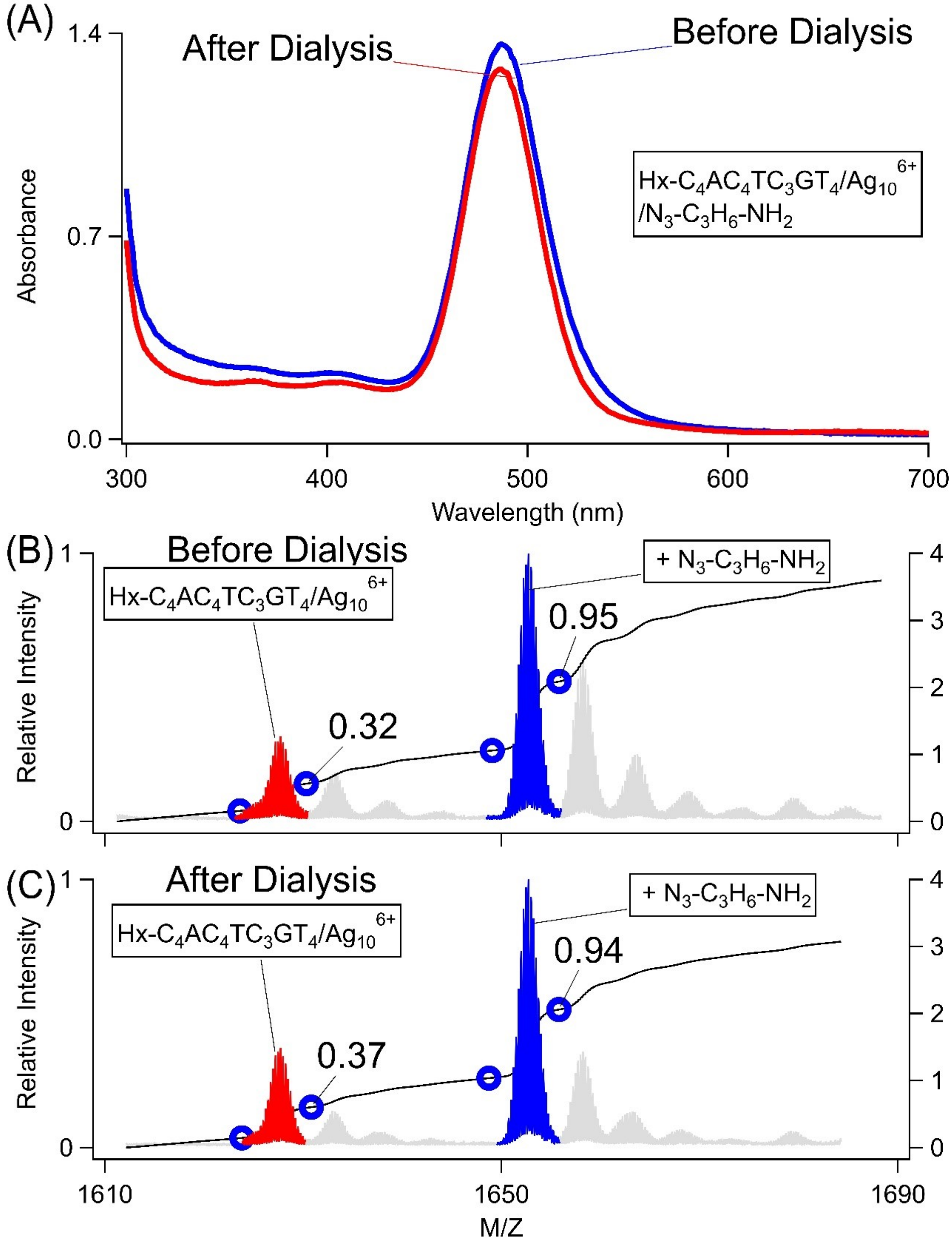

Figure 5S: (A) Absorption spectra before (blue) and after (red) dialysis against 100X volumes of solution. Similar spectra with comparable absorbances suggest that the silvers remain bound to $C_4AC_4TC_3GT_4$ and does not dissociate into the bulk solution. (B) and (C) Mass spectra before (B) and after (C) dialysis against 100X volumes of solution. Similar conversion efficiencies suggest that DNA-bound Ag_{10}^{6+} and not leached silver is responsible for the click reaction.

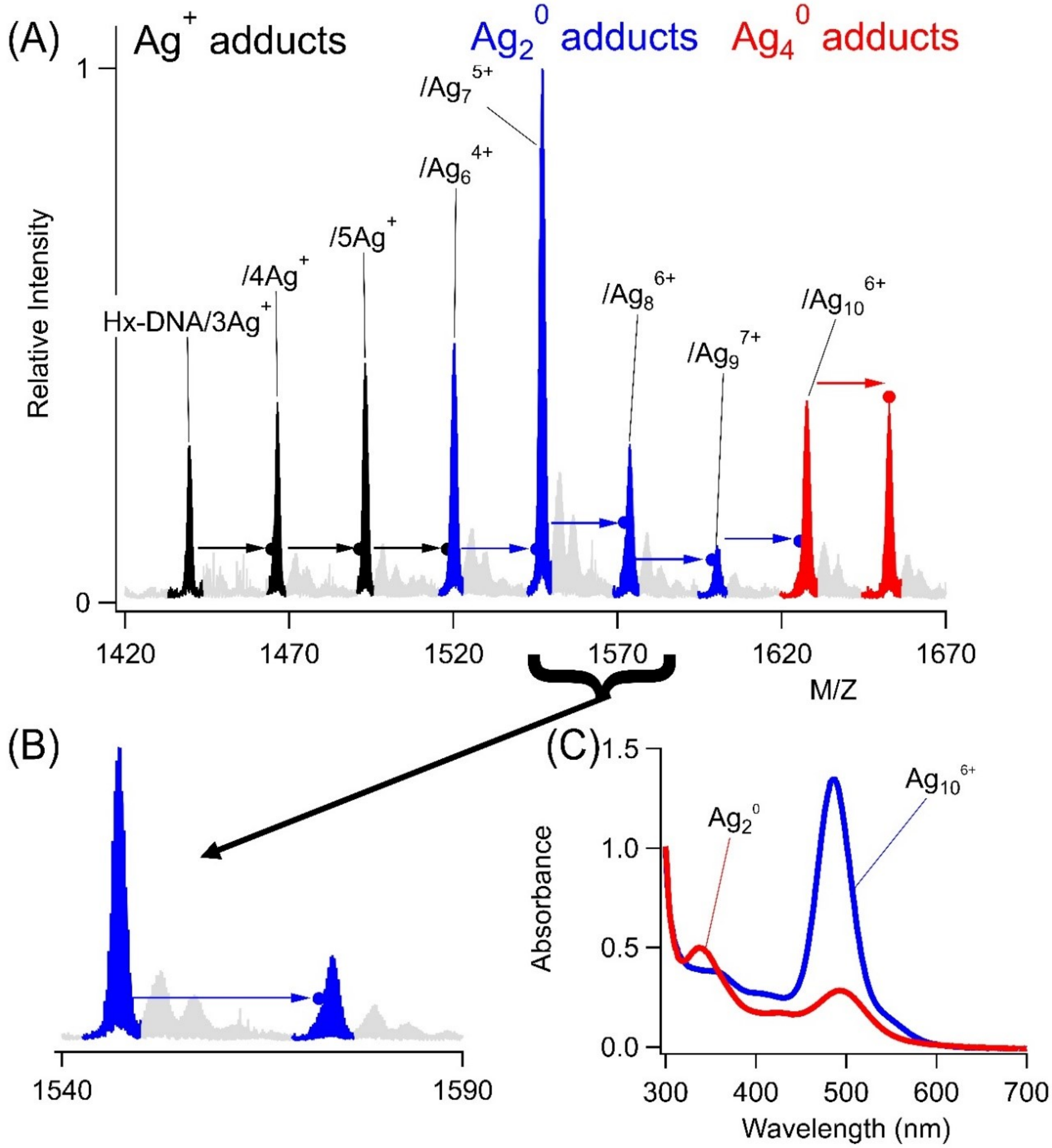

Figure 6S: Mass spectra of irradiated Hx-$C_4AC_4TC_3GT_4$. A series of mixed Ag^+/Ag_2^0 (blue) and purely Ag^+ (black) complexes develop after irradiating Ag_{10}^{6+} (red). After reaction with N_3-C_3H_6-NH_2, the Ag_{10}^{6+} complex converts ~50%, whereas the other complexes show no appreciable conversion. The expected positions of the N_3-C_3H_6-NH_2 products are indicated by arrows and dots. (B) An expanded view of the Ag_7^{5+} complex shows a shoulder that indicates limited conversion that is much less than the Ag_{10}^{6+} complex. (C) Absorption spectra of Hx-$C_4AC_4TC_3GT_4/Ag_{10}^{6+}$ before (blue) and after (red) irradiation using a 490 nm LED at 3 mW for 30 minutes. The 490 nm absorption due to the Ag_4^0 in Ag_{10}^{6+} diminishes while the 335 nm band to a series of Ag_2^0 chromophores develops.

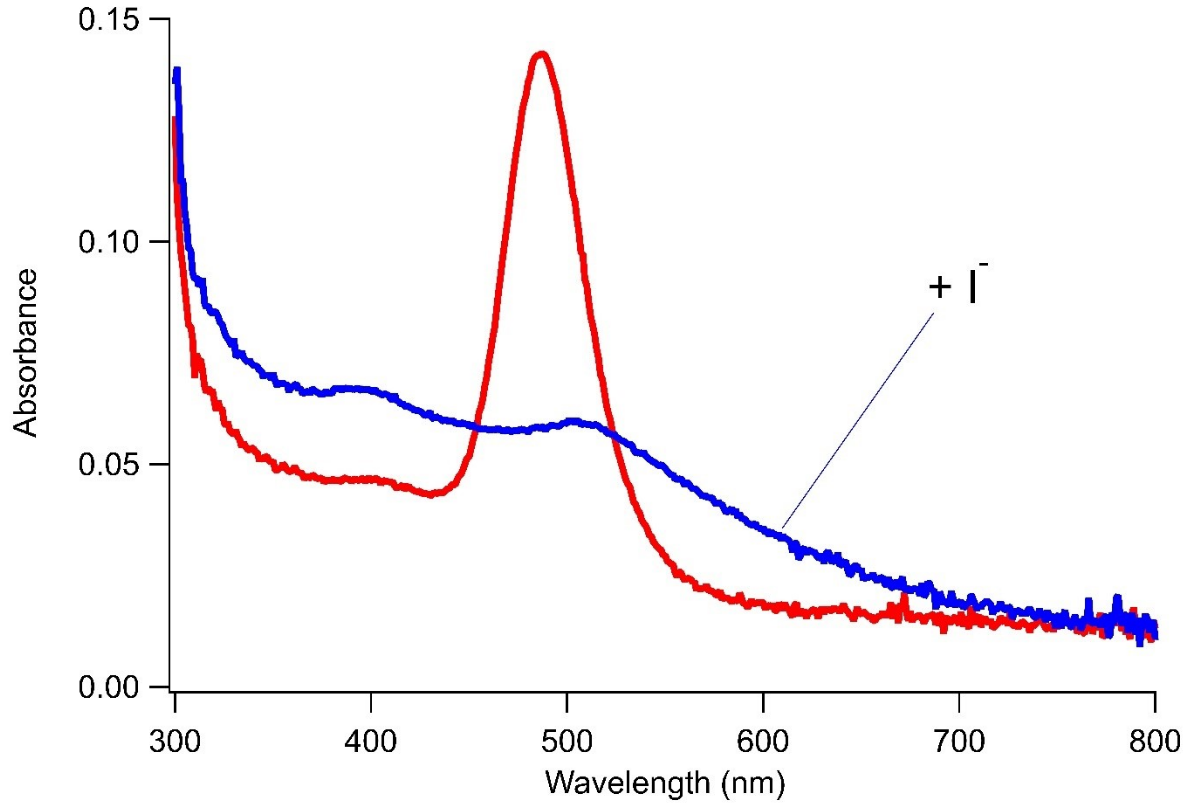

Figure 7S: Absorption spectra of Hx-$C_4AC_4TC_3GT_4/Ag_{10}^{6+}$ before (red) and after (blue) adding 1 equivalent NH_4I:Ag. The loss of the absorption at λ_{max} = 490 nm indicates that the cluster has degraded.

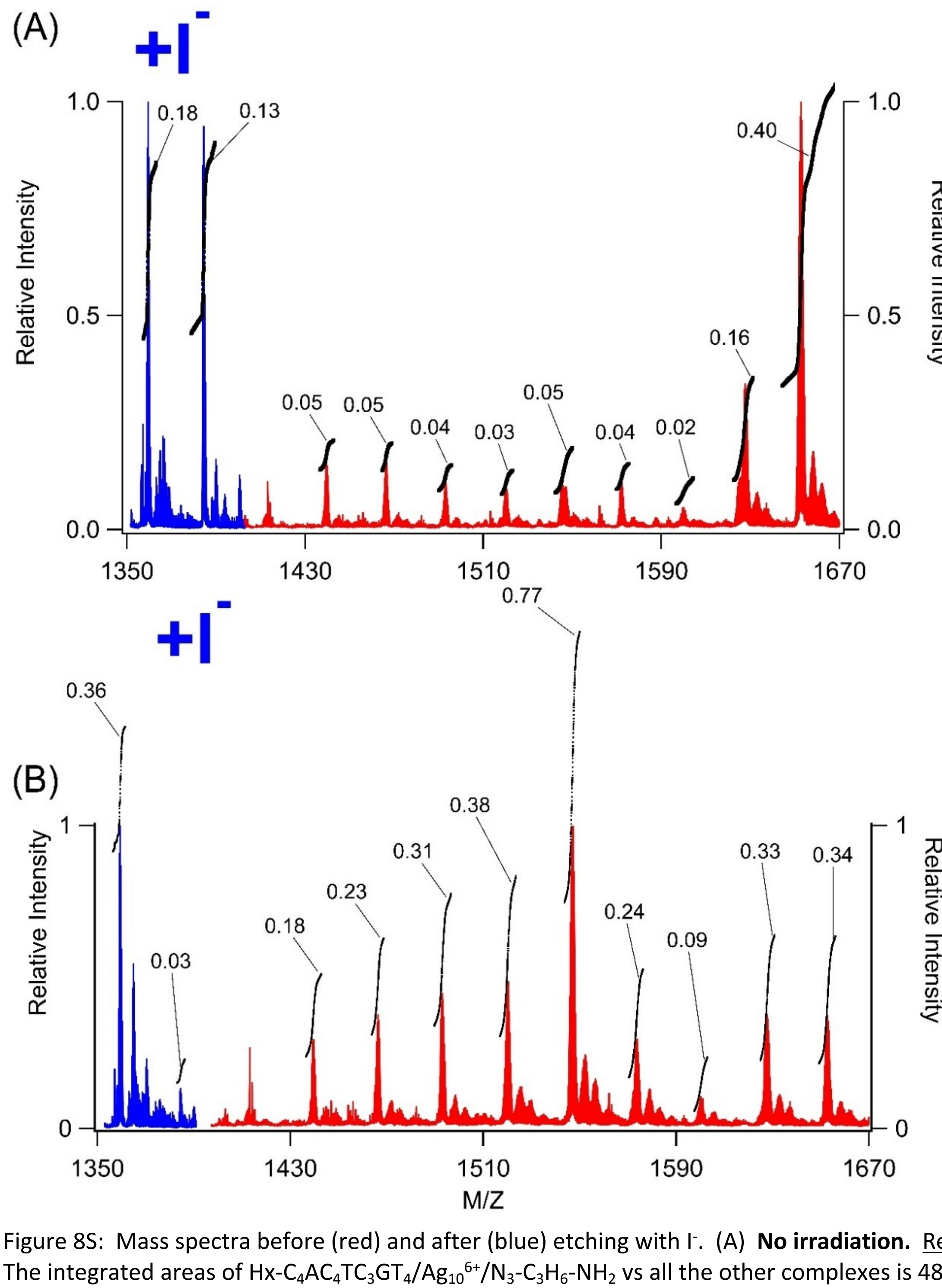

Figure 8S: Mass spectra before (red) and after (blue) etching with I^-. (A) **No irradiation.** Red Peaks: The integrated areas of Hx-$C_4AC_4TC_3GT_4$/Ag_{10}^{6+}/N_3-C_3H_6-NH_2 vs all the other complexes is 48%. Blue Peaks: The integrated areas of Hx-$C_4AC_4TC_3GT_4$/N_3-C_3H_6-NH_2 vs. both strands is 52%. (B) **With irradiation.** Red Peaks: The integrated areas of Hx-$C_4AC_4TC_3GT_4$/Ag_{10}^{6+}/N_3-C_3H_6-NH_2 vs all the other complexes is 12%. Blue Peaks: The integrated areas of Hx-$C_4AC_4TC_3GT_4$/N_3-C_3H_6-NH_2 vs. both strands is 8%.

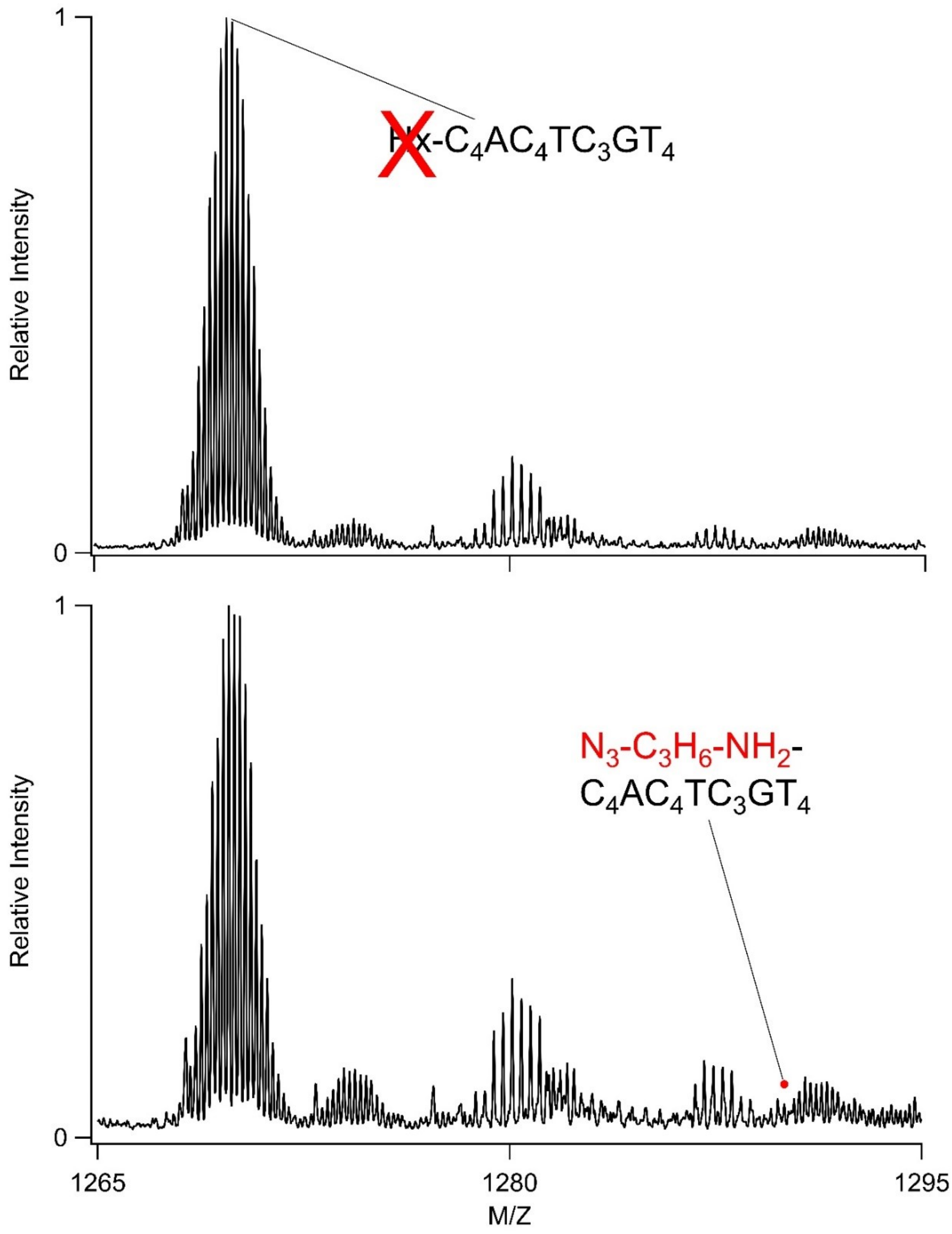

Figure 9S: Mass spectra of $C_4AC_4TC_3GT_4/Ag_{10}^{6+}$ without (top) and with (bottom) 8 equivalents of N_3-C_3H_6-NH_2. The red dot in the bottom spectrum designates the expected M/Z of this adduct. It's absence indicates that the complex is not favored.

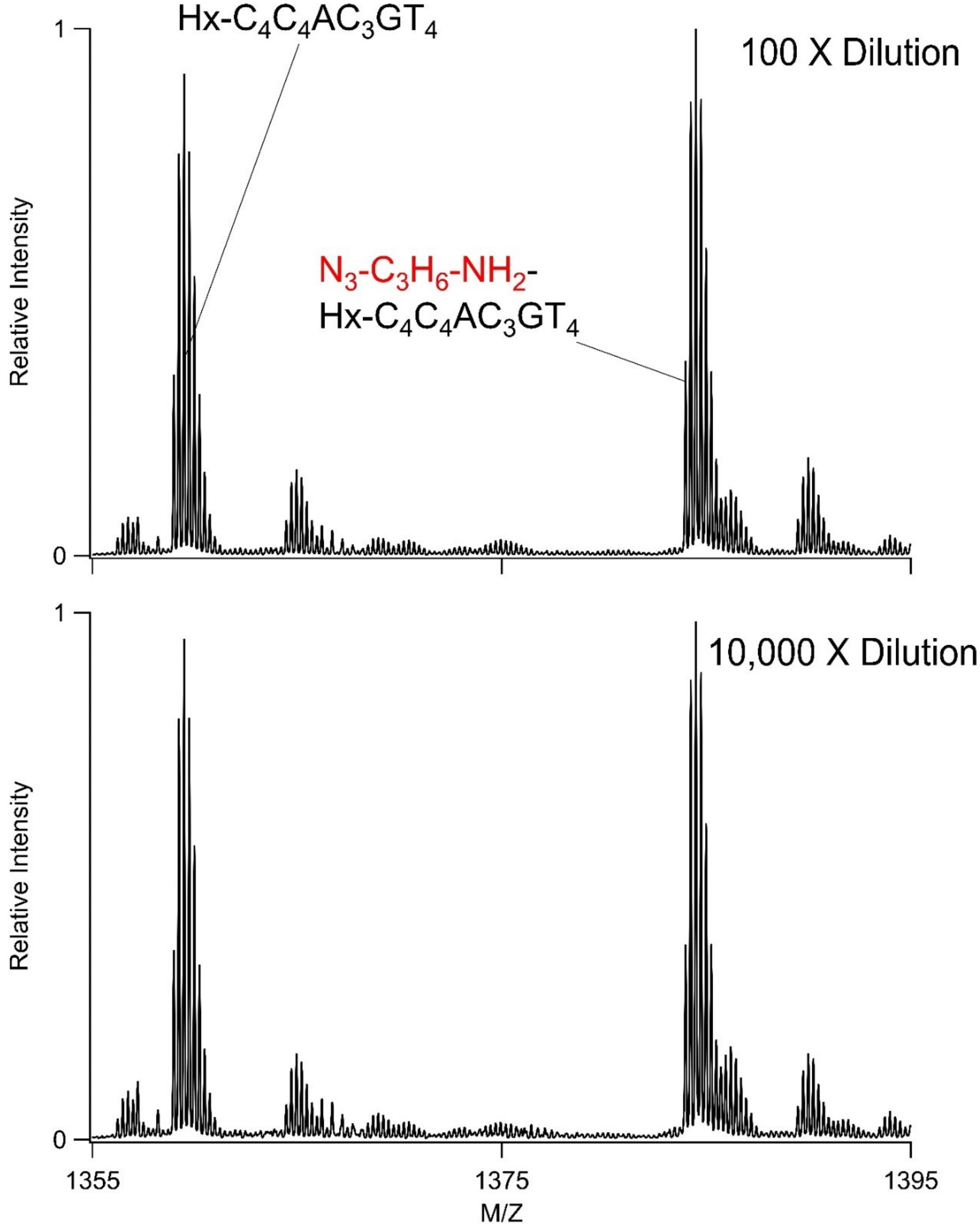

Figure 10S: Mass spectra of the -4 charged state of Hx-$C_4AC_4TC_3GT_4$ without and with the azide N_3-C_3H_6-NH_2 after diluting with 100X (top) followed by another 100X (bottom) volumes of solution. The similarity of the conversion efficiencies suggests that the azide is covalently joined as a triazole.

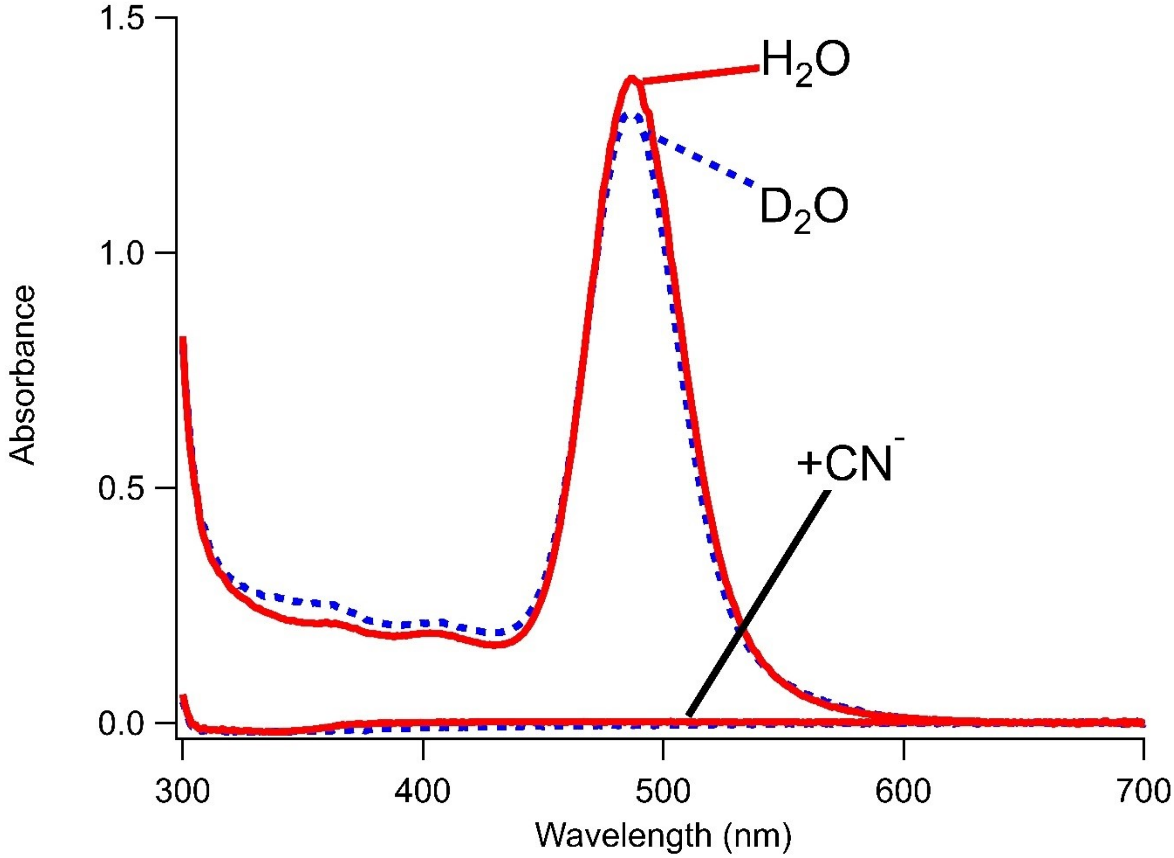

Figure 11S: Absorption spectra of Hx-$C_4AC_4TC_3GT_4/Ag_{10}^{6+}$ in H_2O (solid red) and D_2O (dotted blue) before and after adding 20 equivalents of CN^-. The quenched absorption indicates that the cluster has been removed from the DNA.

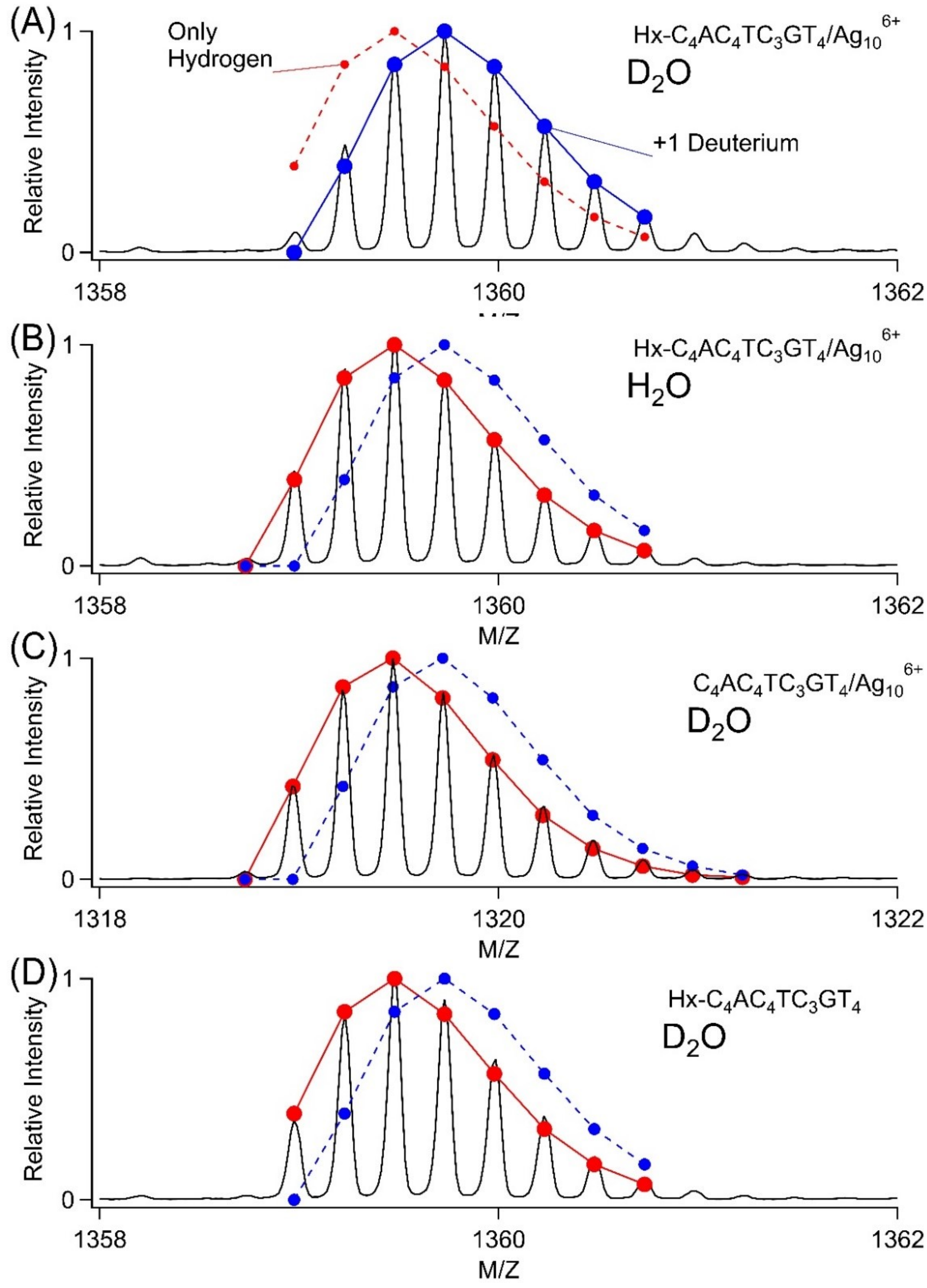

Figure 12S: Comparison of the isotope distributions of Hx-$C_4AC_4TC_3GT_4/Ag_{10}^{6+}$ after etching in D_2O (A), Hx-$C_4AC_4TC_3GT_4/Ag_{10}^{6+}$ after etching in H_2O (B), $C_4AC_4TC_3GT_4/Ag_{10}^{6+}$ after etching in D_2O (C), and Hx-$C_8C_4TC_3GT_4$ in D_2O. Models are based exclusively on hydrogen (red) and hydrogen with 1 deuterium (blue). The model that best describes the data is indicated by a solid line. Only the Hx-$C_4AC_4TC_3GT_4/Ag_{10}^{6+}$ after etching in D_2O is best described by a model with 1 deuterium.

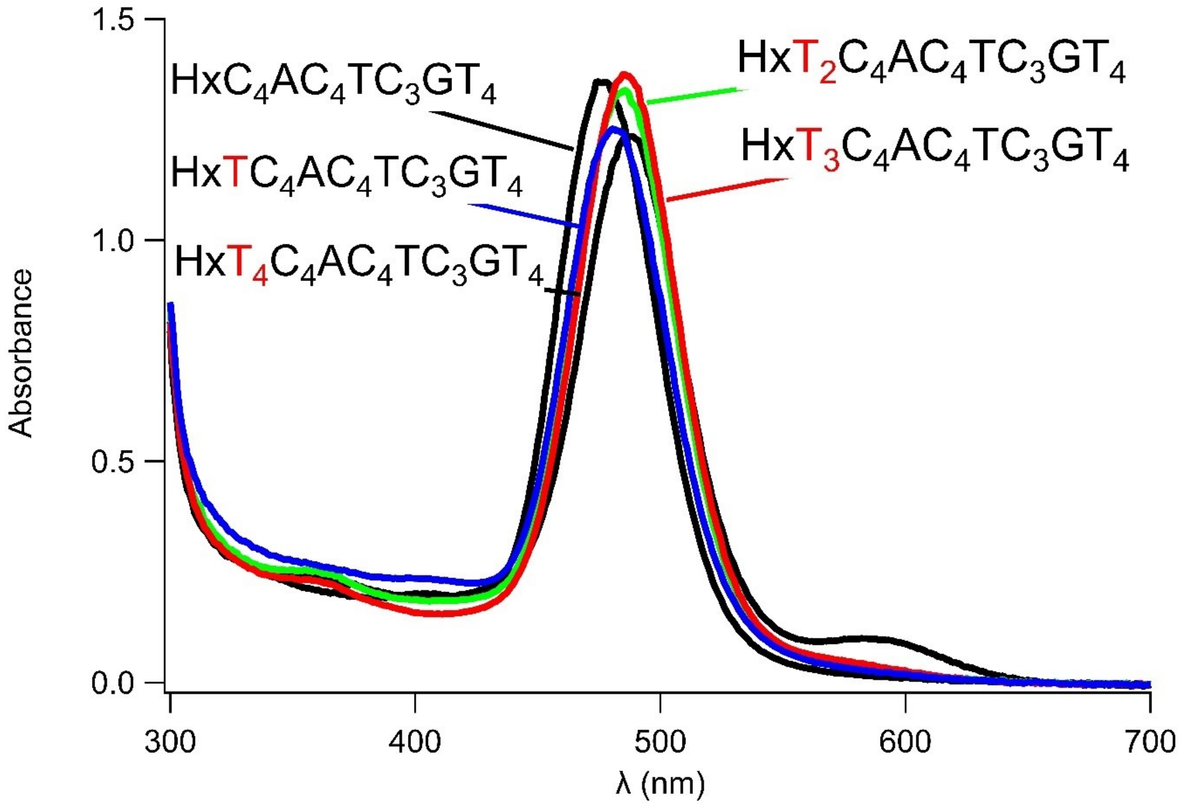

Figure 13S: Absorption spectra of Hx-T_x-$C_4AC_4TC_3GT_4$ strands with x = 0, 1, 2, 3, and 4. Similar λ_{max} and absorbances indicate that the clusters form in similar binding sites.

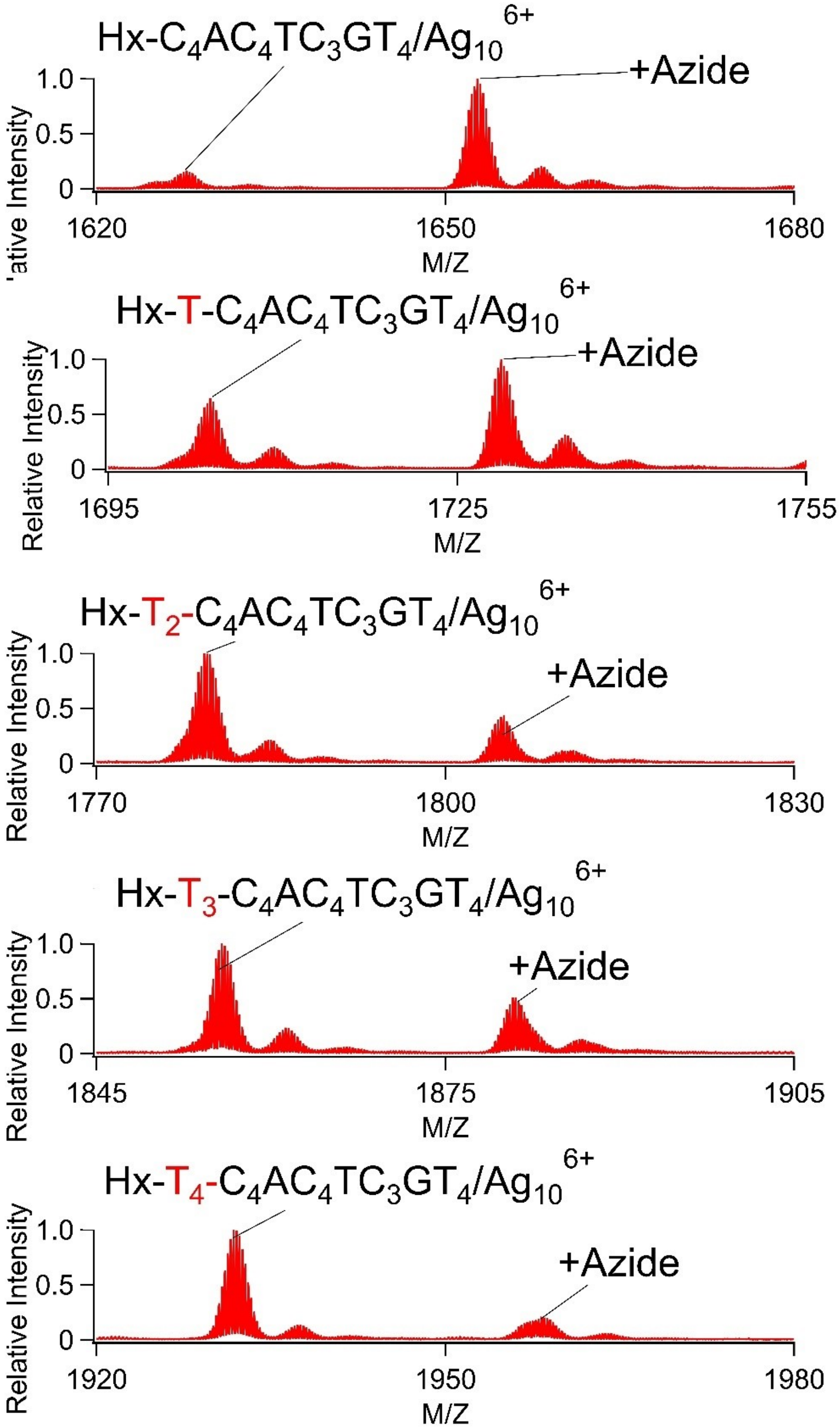

Figure 14S: Mass spectra of Hx-T_x-$C_4AC_4TC_3GT_4$ complexes with x = 0, 1, 2, 3, and 4 respectively. The conversion efficiency decreases as the number of thymines increases.

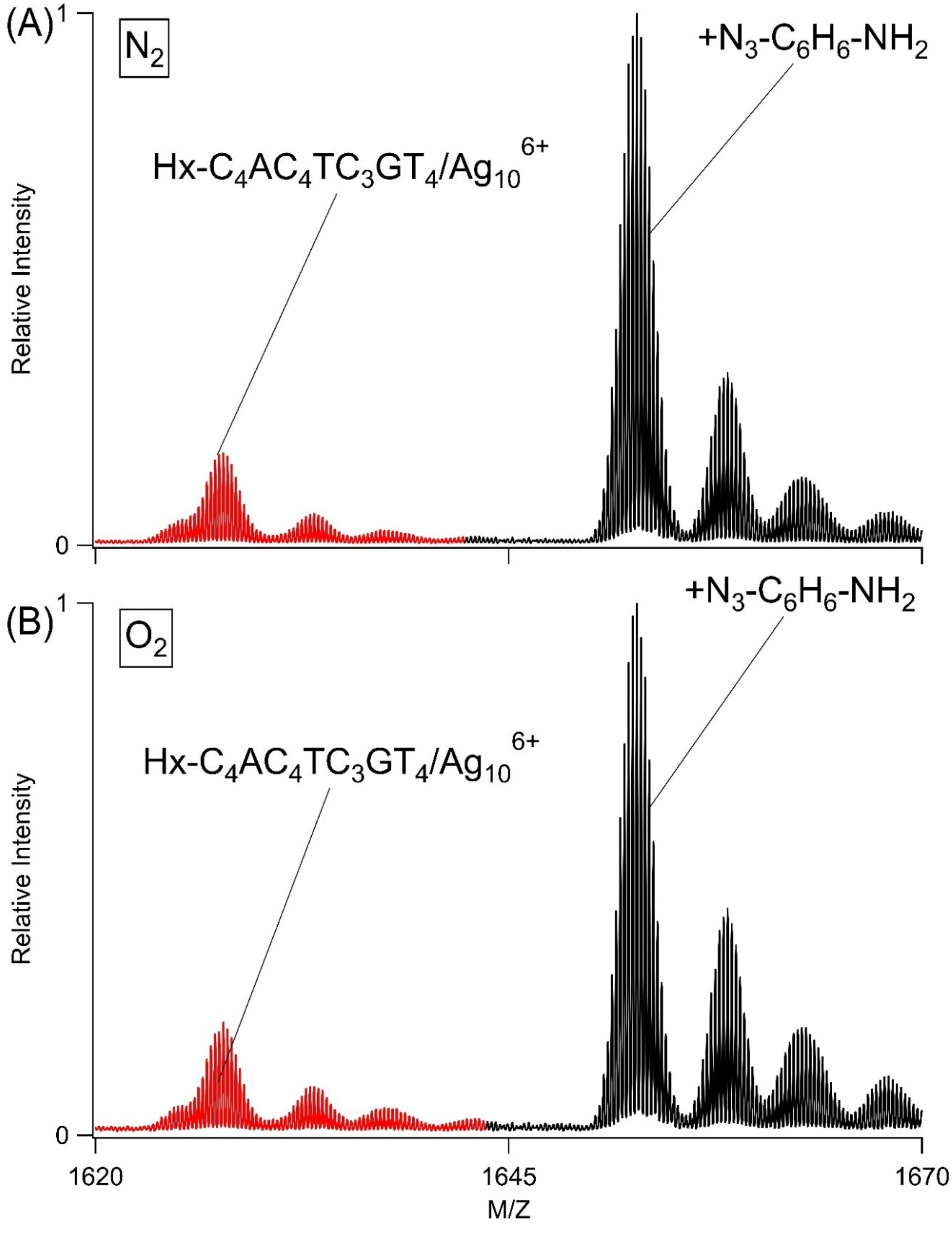

Figure 15S: Mass spectra of the -4 charged ion of Hx-$C_4AC_4TC_3GT_4/Ag_{10}^{6+}$ reacted with N_3-C_3H_6-NH_2 using solutions saturated with N_2 (top) and O_2 (bottom). The similar conversion efficiencies suggest that O_2 does not alter the Ag_{10}^{6+}.

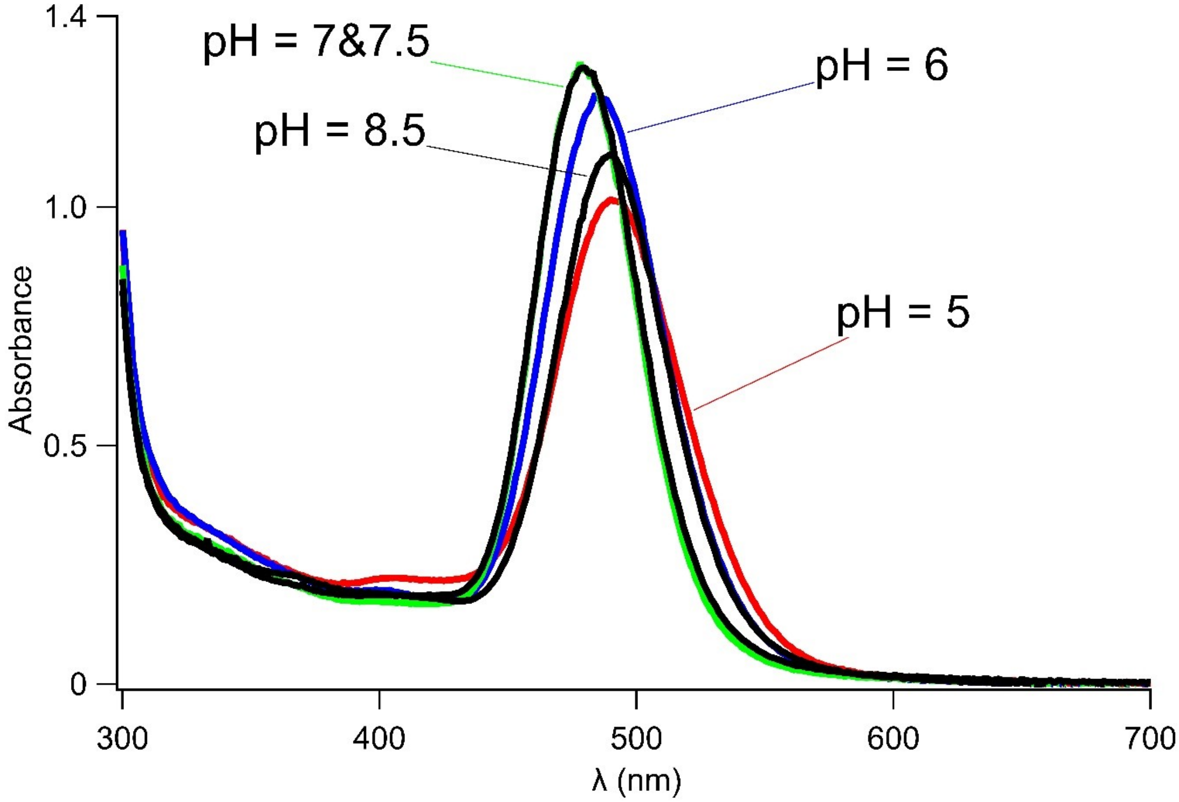

Figure 16S: Absorption spectra of Hx-$C_4AC_4TC_3GT_4/Ag_{10}^{6+}$ in buffers with different pH values. Similar absorbances and spectra indicate similar coordination environments under these conditions.

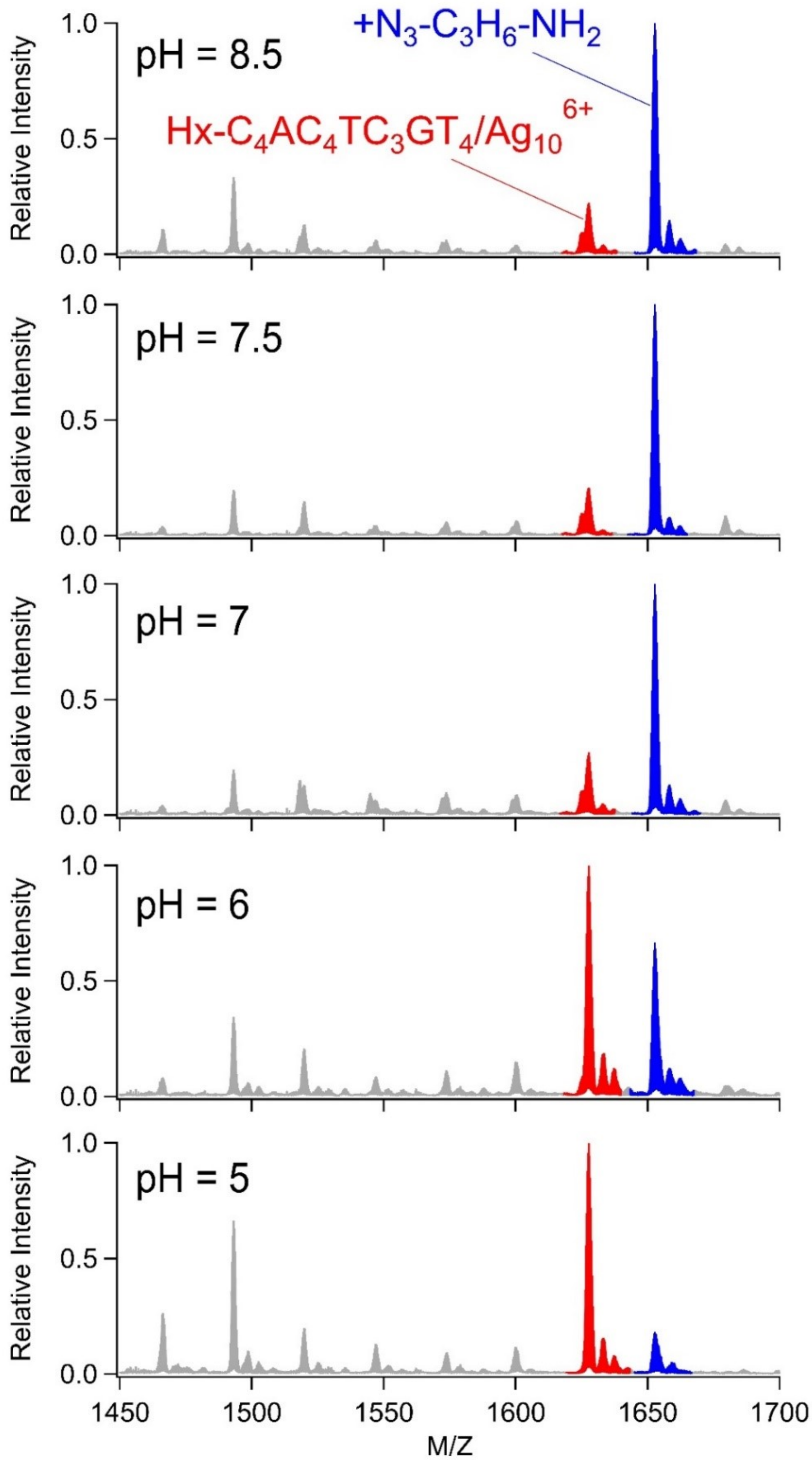

Figure 17S: Mass spectra showing the enhanced conversion efficiency between pH = 6 – 7. The red peaks correspond to Hx-$C_4AC_4TC_3GT_4/Ag_{10}^{6+}$, and the blue peaks correspond to Hx-$C_4AC_4TC_3GT_4/Ag_{10}^{6+}/N_3$-$C_3H_6$-$NH_2$. The conversion efficiencies were 0.18 at pH = 5 and 4.5 at pH = 8.5, thus giving a relative ratio ~25 over this pH range.